Title

Interferon-β induction heterogeneity during KSHV infection is correlated to levels and activation of the transcription factors ATF2 and RelA, and not IRF3

Authors

Machika Kaku[1,2] and Marta Maria Gaglia[2*]

[1]Program in Immunology, Tufts Graduate School of Biomedical Sciences, Boston, MA

[2]Department of Medical Microbiology and Immunology, Institute for Molecular Virology, and Carbone Cancer Center, University of Wisconsin - Madison, WI

ORCIDs: 0000-0002-9921-0678 (M.K.); 0000-0002-1791-0663 (M.M.G.)

[*]Correspondence and reprint requests to Dr. Marta Gaglia, University of Wisconsin-Madison, 1525 Linden Dr, Madison, WI 53706. E-mail address: marta.gaglia@wisc.edu. Phone number: (608)263-5551

Abstract

Careful regulation of type I interferons (IFN) is vital for balancing tissue damage and protection against infections. We previously found that during Kaposi's sarcoma-associated herpesvirus infection, type I IFN induction was limited to a small percentage of infected cells. This heterogeneity was not explained by viral gene expression. Here, we used a fluorescent reporter and fluorescence activated cell sorting to investigate the source of this heterogeneity. Surprisingly, the canonical IFN induction pathway culminating in the activation of the IRF3 transcription factor was similarly activated between cells that made high vs. low/no IFN-β. In contrast, the activation or expression of the two other IFN transcription factors, the NF-κB subunit RelA and the AP-1 subunit ATF2, correlated with IFN-β induction. Our results suggest that during viral infection, activation of IRF3 does not automatically result in IFN responses at the level of individual cells, but that other factors, such as NF-κB and AP-1, are limiting for type I IFN induction.

31 **Importance**

32 The ability of mammalian cells to react to viral infections is a crucial step in the
33 induction of immune responses. The first course of action for the cell is to express and
34 release type I interferons like interferon-β (IFN-β), secreted molecules that warn
35 surrounding cells. Single-cell level examination of gene expression has revealed that
36 surprisingly, during many viral infections, only a small fraction of infected cells makes
37 IFN-β. This is likely a mechanism to prevent immune system overreactions. However, it
38 remains unclear why only some cells respond. Here, we find that during infection with
39 Kaposi's sarcoma-associated herpesvirus, an oncogenic virus that affects
40 immunocompromised individuals, the transcription factors AP-1 and NF-κB, rather than
41 the more commonly studied IRF3, may decide which cells go on to make IFN-β. Our
42 findings contribute to a better understanding of complex gene regulation and shed light
43 on a process that fights an oncogenic virus.

44 **Introduction**

45 Type I and III interferons (IFNs) such as interferon-β (IFN-β) and interferon-λs
46 (IFN-λ) are potent cytokines that defend mammals against viral infections. As a key
47 component of innate immunity, they are induced in response to pathogen-associated
48 molecular patterns (PAMPs), such as nucleic acids with unfamiliar characteristics, or
49 damage-associated molecular patterns (DAMPs) due to infection-induced stress.
50 PAMPs and DAMPs are sensed by pattern recognition receptors (PRRs), leading to IFN
51 induction. Type I and III IFNs then orchestrate antiviral defense by signaling through the
52 IFNAR1/2 and IFNLR1/IL10Rβ receptor complexes, respectively, and induce hundreds
53 of interferon stimulated genes (ISGs) (1). ISGs encode proteins that antagonize viral
54 replication through a variety of mechanisms (2). Despite this crucial antiviral role, IFNs
55 are well known to be a double-edged sword because of their powerful effects on cell
56 and tissue physiology. While insufficient IFN signaling leaves the host susceptible to
57 infections, excessive IFN signaling causes tissue damage and contributes to
58 autoimmune disease development (3-5). Therefore, IFN-β and other type I and III IFNs
59 are carefully regulated, and multiple host regulatory mechanisms have evolved to
60 ensure their expression only under appropriate conditions.

61 An emerging dimension of IFN regulation is transcriptional heterogeneity at the
62 single cell level. This aspect of IFN regulation has become clear from the growing
63 number of single cell RNA sequencing (scRNA-seq) analyses of infected cells. We and
64 others have found only a small percentage (<10%) of virus-infected cells produce IFN-β
65 or IFN-λ (6-18). This has been reported in infections with the RNA viruses Influenza A
66 Virus (7, 10, 11, 14-17), Newcastle Disease Virus (18, 19), West Nile Virus (13), and

67 SARS-CoV-2 (9), as well as the DNA viruses Herpes Simplex Virus 1 (12) and Human
68 Cytomegalovirus (8), and in our studies in Kaposi's sarcoma-associated herpesvirus
69 (KSHV) (6). We had previously discovered that KSHV hijacks the function of host
70 caspases to prevent IFN-β induction when KSHV re-enters the replicative (lytic) cycle
71 from a dormant (latent) infection state (20). Adding a small molecule caspase inhibitor
72 restores activation of the cytoplasmic DNA-sensing PRR cyclic GMP-AMP synthase
73 (cGAS) (6) and results in IFN-β induction (20). The amount of IFN-β produced under
74 these conditions based on ELISA measurements was substantial (20). Nonetheless,
75 subsequent scRNA-seq experiments revealed that the IFN-β comes from a small
76 population of cells, with less than 4% of infected cells producing it even under this
77 "derepressed" condition (6). The limited number of type I/III IFN producing cells across a
78 range of infections and cell types indicate that this is a feature of the IFN induction
79 system.

80 Since subversion of type I IFN is a key evolutionary tactic for viruses in the virus-
81 host arms race, heterogeneity in the expression and activity of IFN-inhibiting viral
82 proteins has been proposed as the reason for heterogeneous IFN-β expression (15,
83 20). However, we and others have found that viral gene expression heterogeneity does
84 not fully explain the observed IFN-β heterogeneity during infection with a range of
85 different viruses – KSHV, Influenza A Virus, Sendai Virus, and Newcastle Disease Virus
86 (6, 11, 19, 21, 22). In our scRNA-seq experiments with KSHV, IFN-β was only detected
87 in cells in the early stages of the KSHV lytic cycle, which made up 46% of the
88 population, indeed suggesting a contribution from viral regulation of IFN (6). Cells that
89 are latently infected with KSHV likely do not detect the infection, while cells in later lytic

90 viral stages have likely shut down host defenses. However, only 6% of the cells in the
91 early lytic stages expressed IFN-β, demonstrating that viral replication stage does not
92 completely determine IFN induction (6). Moreover, when we compared IFN-β positive
93 and negative cells within this population, we did not find any viral gene that was
94 specifically missing in IFN-β-producing cells, as would be expected for a
95 heterogeneously expressed viral IFN suppressor (6). These findings suggested that
96 there is an additional, likely cellular, source of IFN-induction heterogeneity in this
97 system, which may explain the consistency of this phenomenon across viral infections.
98 The host may benefit from limiting the percentage of cells producing IFN-β in an
99 infected population, as this may allow for optimal distribution of the cytokine and
100 protection of surrounding cells without IFNs reaching dangerous levels. However, how
101 IFN induction is restricted to a few cells remains unclear.
102 A potential mechanism could be restricted activation of one of the many signaling
103 steps that are needed for type I and III IFN transcriptional activation downstream of
104 PRRs. While different PRRs rely on different signaling adaptors, their signaling
105 pathways generally converge on the kinase TANK-binding kinase 1 (TBK1), which
106 phosphorylates the key transcription factor interferon regulatory factor 3 (IRF3). While
107 IRF3 activation is commonly used as the main indicator for IFN-β transcription triggered
108 by viral infection, IFN-β transcription also requires additional transcription factor
109 complexes, which together with IRF3 make up the IFN-β enhanceosome: the nuclear
110 factor kappa-light-chain-enhancer of activated B-cells (NF-κB) and the activator protein
111 1 (AP-1) complexes (23). While the AP-1 and NF-κB complexes can be composed of
112 many different members depending on the context, AP-1 complexes formed by c-Jun

113 and ATF2 and NF-κB complexes formed by the RelA/p65 and NFKB1/p50 subunits
114 have been specifically linked to IFN-β transcription during viral infections (24). Previous
115 studies addressing IFN induction heterogeneity have proposed different explanations on
116 how this pathway may result in heterogeneity. Some studies have suggested that
117 promoter firing is inherently stochastic, so that all the components of the induction
118 pathway are active, including the transcription factors, but promoter firing only happens
119 in some cells (19, 25). One study suggested this was due to differences in the 3D
120 structure of the genome (25), while another was unable to pinpoint the source of the
121 noise and concluded it may have to do with enhanceosome assembly (19). In contrast,
122 Zhao et al. proposed that every step leading to IFN induction is subject to
123 heterogeneous noise, from viral replication to signaling protein activation to abundance
124 of transcription factors (21). However, Zhao et al. did not control for the fact that many
125 genes encoding proteins in the IFN induction pathways are themselves ISGs, and this
126 study also used murine cells which do not require NF-κB for IFN induction (21). Overall,
127 the cellular source of the IFN induction heterogeneity remains poorly defined.
128 In this study, we used the KSHV lytic infection and caspase inhibition system to
129 further probe the source of heterogeneous IFN-β induction, as it is a robust and
130 sustained system for inducing IFN in the context of a viral infection. We developed a
131 reporter that allows us to separate cells expressing high vs. low levels of IFN-β and
132 found that surprisingly, the canonical IFN induction pathway culminating in IRF3
133 activation was equally activated in both populations. However, activation or levels of
134 other components of the IFN-β enhanceosome better correlated with IFN-β induction.
135 Thus, in our system, activation of the NF-κB component RelA and baseline levels of the

136 AP-1 component ATF2 may be the limiting factors for IFN-β transcription at the single
137 cell level. Moreover, these findings suggest that that IRF3 serves as the infection signal,
138 while AP-1 and NF-κB provide the barrier to excessive IFN-β, at least in reactivating
139 KSHV-infected BC-3 cells. This study highlights the nuanced mechanics behind the
140 induction of a key component of our body's antiviral response and identifies specific
141 cellular factors that may contribute to limiting IFN-β induction to a small subpopulation of
142 cells during KSHV infection.
143

144 **Results**

145 *A fluorescent tdTomato reporter driven by a minimal human IFN-β promoter*
146 *distinguishes cells that express high vs. low levels of IFN-β*

147 Using scRNA-seq, we previously found that a very small fraction of KSHV-
148 infected cells produce IFN-β when the virus is reactivated and caspases are inhibited
149 (6). In the scRNA-seq dataset, we calculated this fraction to be 3.8% of the total
150 population and 6% of the infected cells in the early stage of the lytic cycle. Nonetheless,
151 the rare IFN-β producing cells clustered together in our scRNA-seq data (6), suggesting
152 that they have different characteristics from other cell populations. To identify factors
153 involved in IFN-β regulation, we sought to separate and compare IFN-β producing and
154 non-producing cells. We previously engineered a tdTomato reporter driven by two
155 copies of the 303 bp minimal promoter sequence from the human *IFNB1* gene (Fig. 1A)
156 and created stable BC-3 cell lines with this reporter (BC3-IFN-βp-tdTomato cells) (6).
157 We did not clonally select the cell line with the intention of focusing on IFN-β promoter
158 sequence as the source of gene induction, and to eliminate contributions from the
159 chromatin location of the reporter or variable reactivation of individual cell clones. BC-3

160 cells are latently KSHV-infected B cells isolated from a patient with primary effusion
161 lymphoma (26). The IFN-β promoter sequence was taken from previous luciferase or
162 chloramphenicol acetyltransferase reporters (27-29). tdTomato was selected because it
163 is the brightest fluorescent protein whose signal is well separated from
164 autofluorescence, which appears in the green channel and is high in BC-3 cells (30-33).
165 While our original scRNA-seq study was performed in KSHV-infected epithelial cells, the
166 iSLK.219 system (6), we chose BC-3s for subsequent experiments because they are
167 more biologically relevant, as B cells, but not epithelial cells, are the target of long-term
168 KSHV infection in patients. Moreover, the virus in iSLK.219 cells expresses GFP and
169 RFP fluorescent reporters (34), which restricts our options for fluorescent markers. In
170 BC-3 cells, the KSHV lytic cycle can be reactivated using the protein kinase C activator
171 TPA. Treating BC3-IFN-βp-tdTomato reporter cells with TPA and the pan-caspase
172 inhibitor IDN-6556 induced tdTomato expression compared to TPA treatment alone,
173 with this expression limited to 2% of the cells when measured by flow cytometry (6).
174 Also, treating BC3-IFN-βp-tdTomato reporter cells with TPA and the pan-caspase
175 inhibitor IDN-6556 induced IFN-β mRNA expression compared to no treatment, TPA
176 alone, or the caspase inhibitor alone (Fig. 1C).
177 To isolate cells expressing high and low IFN-β levels, we subjected the lytically
178 reactivated BC3-IFN-βp-tdTomato reporter cells treated with caspase inhibitors to
179 fluorescence-activated cell sorting (FACS) and collected tdTomato-positive and
180 negative cells (Fig. 1A, B). To confirm that tdTomato-based FACS results in the
181 separation of cells based on IFN-β expression status, we measured tdTomato and IFN-
182 β RNA levels in the sorted samples. Importantly, we found that the endogenous IFN-β

183 transcript was enriched in the tdTomato+ cells and depleted in the tdTomato- cells, as
184 was tdTomato mRNA (Fig. 1D, E). This selective enrichment of both IFN-β and
185 tdTomato transcripts in the sorted cells confirms that the reporter is functional.
186 Moreover, it indicates that the heterogeneity is due to the IFN promoter activity, rather
187 than variable expression due to random insertion of the transgene after lentiviral
188 transduction.

189 Because KSHV reactivation rates can be variable, we confirmed that all our
190 experiments showed robust activation of the lytic cycle by ensuring that a high
191 percentage of cells produced the KSHV lytic protein ORF45 (Fig. 1F) and that there was
192 clear induction of early KSHV lytic gene ORF50 in cells treated with TPA or TPA and
193 caspase inhibitors (Fig. 1G). Sorting for IFN-β high and low cells indicated no correlation
194 between ORF50 and IFN-β expression (Fig. 1H) indicating that lytic cells were found in
195 both populations, as we expected from our previous scRNA-seq results (6). In the
196 scRNA-seq data, we found that KSHV reactivation progression broadly contributes to
197 variable IFN-β induction, since cells with the virus in latency or conversely, in later
198 stages of reactivation did not induce IFN, and all IFN-producing cells appear to be in
199 early stages of KSHV reactivation (6). However, only 6% of the cells in the early stages
200 of viral reactivation induced IFN-β, indicating that progression through the lytic cycle
201 does not fully explain IFN-β heterogeneity (6).

202 While TPA-mediated reactivation is the most commonly used method of reliably
203 reactivating KSHV in primary effusion lymphoma cell lines such as BC-3 cells (35, 36),
204 TPA has other pleiotropic effects such as driving activation of multiple signaling
205 pathways involved in growth, apoptosis, and differentiation in different cell types through

206 activation of protein kinase C (37, 38). Therefore, to ensure that the use of TPA did not
207 confound our studies, we measured IFN induction in an uninfected EBV and KSHV-
208 negative B cell lymphoma line, BJAB cells (39). BJAB cells are commonly used as an
209 uninfected control for experiments with BC3 cells and other primary effusion lymphoma
210 cell lines (40, 41). We found that neither IFN-β nor the type III IFN IFN-λ1 were induced
211 after TPA or TPA and caspase inhibitor (IDN-6556) treatment in uninfected BJAB cells
212 (Fig. 1I, J). Therefore, we concluded that the IFN induction in BC-3 cells was indeed
213 due to KSHV lytic reactivation and virus sensing, not TPA addition, and that this system
214 could be used for further experiments.

215 IFN-β signaling also potentiates its own transcription through upregulation of IFN-
216 induction pathway components (42). Indeed, in the scRNA-seq experiment, blocking
217 IFN responses with an anti-IFN antibody cocktail reduced the number of IFN-β-positive
218 cells (6). Therefore, to specifically analyze the “first responder” cells in which IFN-β was
219 only induced by pathogen sensing, without any feed-forward response, we treated the
220 cells with the anti-IFN antibody cocktail. Consistent with the scRNA-seq results in
221 iSLK.219 cells, we still observed IFN-β induction in the lytic BC-3 cells treated with
222 caspase inhibitors after antibody treatment, although it was decreased (Fig. 2A). FACS
223 based on the tdTomato reporter also successfully enriched the rare IFN-β producing
224 cells under these conditions (Fig. 2B, C). We also still detected reactivation, measured
225 by ORF45 staining or induction of the lytic gene ORF50, in the presence of the antibody
226 cocktail (Fig. 2D, E). Again, sorting for IFN-β high and low cells indicated no correlation
227 between ORF50 and IFN-β expression (Fig. 2F).

228 The enrichment of IFN-β mRNA in cells selected for tdTomato expression (with
229 and without blocking IFN paracrine signaling) demonstrates that our IFN-βp-tdTomato
230 reporter recapitulates heterogeneous expression of the native IFN-β transcript. High
231 levels of reporter expression corresponded to high levels of IFN-β mRNA. Moreover,
232 these results demonstrate that FACS of the BC3-IFN-βp-tdTomato reporter line allows
233 us to separate cells producing high and low levels of IFN-β within a population and to
234 analyze differences between them.
235
236 *IFN-β is not stochastically induced*
237 Some groups have proposed that heterogeneous expression of IFN-β may be
238 generated by stochasticity of IFN-β promoter firing (19, 25). This model posits that the
239 signals and activated proteins needed for IFN-β induction are present in all infected
240 cells, but transcription of IFN-β only occurs stochastically in some cells. To test this
241 hypothesis, we took advantage of the fact that pathogen sensing often induces type III
242 IFNs like IFN-λ1 in addition to type I interferons. The signaling cascade and
243 transcription factors that regulate IFN-β and IFN-λ1 are largely the same (43), so any
244 heterogeneity in upstream signaling should affect their induction in a coordinated way
245 (Fig. 3A). The IFN-β promoter is bound by AP-1, IRF3, and NF-κB, and the IFN-λ1
246 promoter by IRF3 and NF-κB (44). However, since IFN-β and IFN-λ1 have separate
247 promoters and are located on different chromosomes, stochastic noise in assembly of
248 the transcription factors or other aspects of promoter firing (19) would differentially affect
249 them. Contrary to the stochasticity model, our results suggested that IFN-β and IFN-λ1
250 were induced in the same cells. In the previously published scRNA-seq results, IFN-λ1
251 was also induced in iSLK.219 cells upon lytic reactivation and caspase inhibitor

252 treatment, and in the same rare cell populations that expressed IFN-β, indicating a
253 shared regulation mechanism (6). We have since performed further analysis of the
254 scRNA-seq data and found that indeed expression of IFN-λ1 and IFN-β were highly
255 correlated at the single cell level. In fact, no other transcript showed closer correlation
256 using Seurat function for gene enrichment, FindAllMarkers, on single cells separated by
257 IFN-β expression. We also analyzed IFN-λ1 expression after sorting BC3-IFN-βp-
258 tdTomato cells, using the same samples in which we analyzed IFN-β expression in Fig.
259 1. Like IFN-β, IFN-λ1 was induced in BC-3 lytic cells treated with the caspase inhibitor
260 IDN-6556 (Fig. 3B). Moreover, IFN-λ1 was enriched and depleted in concert with IFN-β
261 in the tdTomato positive and negative cells, respectively (Fig. 3C. compared to IFN-β in
262 the same samples, Fig. 1D). This result indicates that IFN-β and IFN-λ1 were expressed
263 in the same subset of cells. Similarly to IFN-β, IFN-λ1 induction can also be potentiated
264 in response to IFN signaling by a feed-forward loop (Fig. 3A), so we repeated the
265 experiments in the presence of anti-IFN antibodies to block paracrine signaling and
266 checked that the correlation was not a response to IFN. While this treatment did reduce
267 IFN-λ1 induction dramatically, the pattern of IFN-λ1 and IFN-β co-expression was also
268 observed in the absence of IFN responses, as the IFN-λ1 transcript was enriched in the
269 tdTomato+ cells (Fig. 3E), where IFN-β was also enriched (Fig. 2B, same samples).
270 These results stand in contrast to MxA, a classical ISG. MxA is induced in the lytically
271 reactivated and caspase inhibitor-treated cells (Fig. 3F), i.e. under conditions where
272 IFNs are secreted, as expected for an ISG. Moreover, also as expected, anti-IFN
273 antibodies block MxA induction (Fig. 3H; anti-IFN antibodies were only added to the lytic
274 + caspase inhibitor condition, as this is the condition in which we see high IFN

275 production). This result also confirms that the antibody treatment blocks IFN responses.
276 However, unlike IFN-λ1, MxA is not enriched in sorted cells in the presence or absence
277 of paracrine signaling, demonstrating that the coordinate expression of IFN-λ1 and IFN-
278 β was not related to IFN responses and IFN signaling potentiation of IFN-λ1 induction
279 (Fig. 3G, I). These results are consistent with the scRNA-seq data in iSLK.219 cells,
280 where we detected IFN-induced ISG expression in all cell clusters, not just the ones
281 producing IFN-β, whereas IFN-λ1 was mostly detected in IFN-β-producing clusters (6).
282 Therefore, we conclude that IFN-β and IFN-λ1 are not stochastically transcribed but
283 coordinately regulated. Moreover, the fact that they are expressed in the same rare
284 subset of KSHV-infected cells suggests that heterogeneity in the same upstream
285 determinants leads to cell-to-cell differences in type I and III IFN induction.
286
287 *TBK1 and IRF3 activity does not explain IFN-β heterogeneity*
288 The results above suggested that activation of the IFN-β induction pathway,
289 rather than IFN-β transcription, was heterogeneous. However, there are several
290 signaling steps in the IFN-β induction pathway that could be the bottleneck determining
291 whether cells transcribe IFN-β. Therefore, we monitored activation of the IFN-β
292 induction pathway, particularly the later steps of kinase and transcription factor
293 activation. Using inhibitors for cGAS and TBK1, we confirmed IFN-β and IFN-λ1
294 induction is driven by the cGAS-STING pathway through the TBK1 kinase in KSHV-
295 reactivating BC-3 cells (Fig. 4A, B), similarly to what we had previously found in the
296 epithelial iSLK.219 cells (6, 20). We thus tested whether TBK1 was activated only in the
297 cells that induced IFN-β by comparing levels of TBK1 phosphorylation in lytically

298 reactivated, caspase inhibitor-treated cells sorted based on tdTomato status. To ensure
299 the antibodies detected the correct epitopes, we used poly(I:C)-treated A549 cells as
300 positive controls for TBK1 phosphorylation. In every experiment, tdTomato-based
301 sorting resulted in the expected enrichment and depletion of IFN-β mRNA in tdTomato+
302 and tdTomato- cells, respectively (RNA measurements are shown in Fig. 1D). However,
303 surprisingly, we observed no difference in activated (phosphorylated) TBK1 between
304 IFN-β high and low cells (Fig. 4C, D). Since TBK1 phosphorylates and activates the
305 well-characterized IFN-β transcription factor IRF3, we also tested whether IRF3 was
306 differentially activated in the IFN-β high vs. low cells (i.e. tdTomato+ and -), again using
307 poly(I:C)-treated A549 cells as a positive staining control. Like TBK1, we observed no
308 difference in IRF3 phosphorylation between the two populations (Fig. 4C, E). We also
309 observed no difference in TBK1 and IRF3 phosphorylation between IFN-β high and low
310 cells when we blocked autocrine and paracrine IFN-β signaling with anti-IFN antibodies
311 (Fig. 4F-H). All these experiments were conducted on samples in which we had verified
312 IFN-β mRNA enrichment in the tdTomato+ sorted cells (Fig. 2B). Therefore, while both
313 TBK1 and IRF3 were active in lytic cells treated with caspase inhibitors, their activation
314 alone was not predictive of IFN-β induction. To ensure that the lytic cycle-inducing TPA
315 treatment was not a confound for these experiments, we treated uninfected BJAB cells
316 with the same drugs (TPA and the caspase inhibitor IDN-6556). We confirmed that
317 these treatments did not activate TBK1 and IRF3 in the absence of KSHV infection (Fig.
318 4I). These results indicate that the canonical IFN induction pathway is activated in
319 many, likely most, lytically reactivated KSHV-infected BC-3 cells when caspases are

320 inhibited. However, an additional factor besides IRF3 activation keeps IFN-β induction
321 limited to a small fraction of the population.
322
323 *Expression of the AP-1 subunit ATF2 and activation of the NF-κB subunit RelA correlate*
324 *with IFN-β induction and may drive heterogeneity*
325 IRF3 activation is assumed to lead to IFN-β transcription, and phosphorylation of
326 IRF3 is commonly used as a proxy for IFN induction. However, the IFN-β
327 enhanceosome contains two additional transcription factor complexes: AP-1, composed
328 of c-Jun and ATF2, and NF-κB, composed of RelA/p65 and NFKB1/p50 (Fig. 5A) (24,
329 45, 46). NF-κB and IRF3 are also verified transcription factors for IFN-λ1 (47). How AP-
330 1 and NF-κB are activated during IFN-β induction and their relation to activation of
331 cGAS and other PRRs is not well understood. Given that IRF3 activation did not explain
332 IFN-β heterogeneity, we considered the possibility that AP-1 and/or NF-κB might be
333 determinants of heterogeneous IFN-β induction in our system. We previously reported
334 that expression of NF-κB family members were enriched in IFN-β-expressing cells
335 based on single cell RNA-seq analysis of KSHV-infected epithelial cells treated with
336 caspase inhibitors (6). We reanalyzed the scRNA-seq dataset to test whether this was
337 also the case for the AP-1 components. To further explore the relationship between
338 IFN-β and these transcription factors, we separated the cells from the two IFN-β
339 expressing clusters by IFN-β status. The AP-1 component ATF2 was enriched in both
340 IFN-β-positive and negative cells within the IFN-β expressing clusters, while the AP-1
341 component c-Jun and the NF-κB components RelA and NFKB1 were specifically
342 enriched in the IFN-β-positive cells (Fig. 5B). These enrichments were particularly

343 evident when anti-IFN antibodies were added to block paracrine and autocrine
344 signaling, because most of these genes were also induced by IFN-β signaling (Fig. 5C).
345 To note, there was an enrichment of IRF3 mRNA in the IFN-β-producing cells in the
346 scRNA-seq data (Fig. 5B-C), even though we did not detect enrichment at the protein
347 level in BC-3 cells (Fig. 4C, F). We also observed that after blocking paracrine signaling,
348 IFN-β expression was reduced in one of the IFN-β expressing clusters (Fig. 5B-C). This
349 cluster may represent “secondary responder” cells in which IFN-β is induced mainly
350 after the initial IFN signaling potentiates the sensitivity of the cells, while the other
351 cluster may comprise “first responder” IFN-β-producing cells (Fig. 3A). These results are
352 consistent with the overall reduction in IFN-β induction that we saw upon addition of the
353 anti-IFN antibodies (Fig. 2A).

354 We then tested whether NF-κB and AP-1 were similarly enriched at the protein
355 level in BC-3 cells expressing high levels of IFN-β. To reduce confounds from paracrine
356 signaling observed in the scRNA-seq results, we performed the FACS experiments with
357 anti-IFN blocking antibodies. Interestingly, we observed an enrichment in the AP-1
358 component ATF2 in tdTomato+ cells, indicating that ATF2 levels are higher in cells that
359 express high levels of IFN-β (Fig. 5D, E). Total ATF2 levels did not change between
360 conditions in bulk samples, indicating that ATF2 expression was not induced at the bulk
361 level during infection and/or by caspase inhibitor treatment. Instead, these results
362 suggest that basal expression of ATF2 may be variable and that IFN-producing cells
363 had higher ATF2 levels prior to lytic reactivation (Fig. 5D). It is also possible that ATF2
364 levels are upregulated only in the rare cells that express IFN. ATF2 levels were not
365 changed by TPA and/or caspase inhibitor treatment in uninfected BJAB cells (Fig. 5G).

366 Levels of the other AP-1 component, c-Jun, were variable across replicates, but in two
367 out of three replicates a unique shorter isoform was detected in the sorted IFN-β high
368 cells (Fig. 5D). However, this shorter c-Jun isoform was also induced by treatment of
369 uninfected BJAB cells treated with TPA and caspase inhibitors, suggesting that its
370 appearance may be unrelated to viral replication and IFN induction (Fig. 5H), as IFN-β
371 is not induced in uninfected cells (Fig. 1K). In addition, we also found that IFN-β high
372 cells are enriched in phosphorylated RelA, one of the NF-κB components, whereas
373 there was little to no phosphorylated RelA in the IFN-β low cells (Fig. 5I-J). This result
374 points to RelA activation only in IFN-β high cells. RelA phosphorylation was not induced
375 by TPA and/or caspase inhibitor treatment in uninfected BJAB cells at the same
376 timepoint (two days after TPA addition), indicating this was specific to infected cells (Fig.
377 5K). Overall, these results indicate that ATF2 and p-RelA likely have important roles in
378 cell-specific IFN-β induction. Particularly elevated ATF2 levels may be needed for IFN-β
379 induction, while RelA is likely activated in response to a stimulus to potentiate IFN
380 transcription in the small subset of IFN producing cells (Fig. 6).
381

382 **Discussion**

383 In this study, we investigated underlying differences between cells that induce
384 high vs. low levels of IFN-β in the context of KSHV infection and caspase inhibition. We
385 reveal that the IFN-β enhanceosome components AP-1 and NF-κB, but not IRF3, are
386 likely to determine whether individual cells induce IFN-β during KSHV and caspase
387 inhibition. Protein levels of the AP-1 factor ATF2 and phosphorylation of the NF-κB
388 factor RelA were higher in cells that express higher levels of IFN-β compared to cells
389 that express low IFN-β. ATF2 levels were not upregulated under IFN-inducing

390 conditions in bulk samples, suggesting that sorting for cells with high IFN-β enriched for
391 cells with high ATF2. Therefore, this result points to a model whereby ATF2
392 heterogeneity precedes viral reactivation, and only cells with higher ATF2 respond to
393 pathogen cues by turning on IFN-β. In contrast, RelA was only activated under IFN-
394 inducing conditions, which suggests a possible bottleneck to its activation in most cells.
395 Our findings thus support a model in which IFN-β inducibility during KSHV lytic
396 replication is limited to a rare fraction of cells with elevated baseline ATF2 levels and
397 activated NF-κB. While IRF3, AP-1, and NF-κB have long been known to regulate IFN
398 transcription, the cell-to-cell heterogeneity in their levels and activation has not
399 previously been reported. Moreover, this is the first description of a possible role for AP-
400 1 and NF-κB in controlling which individual cells make IFN, despite cGAS-to-IRF3
401 signaling being active in almost all infected cells in the population.

402 Host regulation of IFN-β is important given its potent effects on both the host and
403 pathogen through autocrine and paracrine induction of hundreds of ISGs. Insufficient
404 induction of ISGs can lead to susceptibility to infection, while excessive IFN-related
405 inflammation can lead to autoimmune disorders and excessive tissue damage. A
406 system in which the barrier for IFN-β induction is very high may provide an appropriate
407 level of innate immune alarm by limiting IFN-β expression to a small fraction of infected
408 cells. The fact that many viral infections display heterogeneous IFN induction in a way
409 that is not fully explained by viral factors (11, 19, 21, 22), in combination with our
410 results, suggests that an important part of the mechanism of IFN regulation is rooted in
411 cellular heterogeneity. Furthermore, heterogeneous expression of other cytokines such

412 as IL-2 (48), IL-4 (49, 50), IL-5 (51), and IL-10 (52) has been reported, suggesting this is
413 an important mode of immune regulation.

414 Interestingly, while IRF3 and TBK1 are required for IFN induction following
415 PAMP/DAMP signaling, here we found they are not sufficient for IFN-β induction.
416 Moreover, this result shows that heterogeneity in the presence of the PAMP/DAMP
417 stimulus, which in our system is likely mitochondrial DNA (unpublished data), cannot
418 explain IFN induction heterogeneity. Although IRF3 activation is often used as a proxy
419 for IFN-β induction, especially in studies of viral infections, our results indicate that this
420 one-to-one relationship is not true at the level of individual cells. Indeed, both TBK1 and
421 IRF3 appear to be activated regardless of the IFN-expressing status of the cells. Most
422 likely, the upstream components of the IFN induction pathway, including the PRR
423 (cGAS in this case), are also activated regardless of the IFN status of the cells. Instead,
424 our results point to the other IFN-β enhanceosome factors, AP-1 and NF-κB, as the
425 potential limiting factors that determine IFN-β induction in individual cells. We propose a
426 model where activation of IRF3 is the main signal that reports on the presence of an
427 infection, while the main function AP-1 and NF-κB is to provide an additional barrier to
428 limit IFN-β induction to a small subset of cells among an infected population.

429 The regulation of AP-1 and NF-κB during IFN responses is not as well
430 characterized as the activation of IRF3. For AP-1, our results suggest that differences
431 may precede infection, because at the bulk level there is no clear change in ATF2
432 levels. Therefore, the simplest interpretation for our results (Fig. 5D) is that some cells
433 have higher ATF2, and these cells are more abundant in the IFN-producing pool. We
434 were unable to detect changes in phosphorylation of ATF2 and c-Jun under IFN-

435 inducing conditions, suggesting this activation step may be dispensable in our system
436 (data not shown). In contrast, NF-κB is likely activated in a subset of cells under IFN-
437 inducing conditions. While IRF3 and NF-κB may both be activated downstream of
438 STING based on previous studies (53, 54), the fact that NF-κB is only phosphorylated in
439 IFN-β high cells while IRF3 is also phosphorylated in IFN-β low cells indicates that there
440 must be a heterogenous bottleneck specifically for NF-κB activation. We attempted to
441 use inhibitors of the IκB kinases α and β (IKKα/β), which activate RelA under other
442 conditions (55-57), to test whether they are required for RelA phosphorylation and IFN-β
443 induction in KSHV infection. However, IKKα/β inhibitors strongly inhibited KSHV
444 reactivation (data not shown), which precluded testing of effects on IFN-β induction. We
445 also tested inhibitors of the transforming growth factor-β-activated kinase 1 (TAK1),
446 which, in many signaling pathways, is upstream of IKKα/β (58), but this inhibitor had no
447 effect on IFN-β levels or phosphorylation of RelA in our system (data not shown).
448 Therefore, we still do not know whether IKKα/β or other kinases phosphorylate NF-κB
449 during IFN-β induction in our system.

450 While this study has shed light on the expression mechanics of IFN-β during
451 KSHV infection, it is possible that the mechanism of IFN heterogeneity is different for
452 other viral infections and cell types. Although IFN heterogeneity is a widespread feature
453 of viral infection, reported by every study we have encountered, the PRRs and signaling
454 pathways that lead to IFN induction vary (6-18, 59). Moreover, IFN-β expression
455 patterns appear to differ between cell types. For example, a larger proportion of
456 dendritic cells express IFN-β upon infection (19, 60, 61) compared to other cell types
457 such as fibroblasts and epithelial cells (6-16). Flexibility in tailoring the IFN response to

458 factors such as cell type, viral load, and PAMP type is likely evolutionarily beneficial in
459 mounting an appropriate immune response. More studies identifying the determinants of
460 IFN expression are needed to parse out the ubiquity vs. uniqueness of our findings.
461 Although our findings suggest there is a high barrier to IFN-β induction, results
462 from studies using Sendai virus suggest that heterogeneity of IFN-β induction is not due
463 to a complete inability of some cells to induce IFN-β. Infection with a highly inflammatory
464 strain of Sendai virus (Cantell) induced IFN-β expression in 99% of infected A549 cells
465 at high multiplicity of infection (11, 61). In comparison, only 0.48% of A549 cells
466 expressed IFN-β during infection with influenza A virus (11). This indicates that IFN-β
467 regulation can be overridden given excessive stimuli such as the defective-interfering
468 viral genomes that characterize the Sendai virus strain Cantell (62). These observations
469 also suggest that the strength or abundance of the stimulus may matter. Indeed, strong
470 IFN inducers like Newcastle Disease Virus, Sendai virus strain Cantell, or the potent
471 PAMP mimetic poly(I:C) induce IFN-β in a larger proportion of cells (10-99%) (21, 22,
472 59, 60, 63-66) compared to other viral infections and treatments (1-10%) (6-17).
473 Unfortunately, we have been unable to test whether the relationship between stimulus
474 strength and percentage of IFN-expressing cells is also true in KSHV-reactivating BC-3
475 cells, as we have not identified a stronger stimulus for these cells. To isolate the cells
476 that express IFN-β, the cells need to be active and viable for long enough for the
477 tdTomato fluorescent protein to express and accumulate to detectable levels.
478 Commonly used IFN-inducing stimuli (poly(I:C), 2’3’-cGAMP, STING agonist diABZI,
479 TLR7 agonist imiquimod, and plasmid DNA) either did not induce IFN-β expression in
480 BC-3 cells or induced cell death before we could measure tdTomato production (data

481 not shown). IFN-β induction through KSHV reactivation and caspase inhibition allows for
482 sustained IFN-β induction without inducing cell death, which gives us a unique tool to
483 study the elusive phenomena of cellular heterogeneity during IFN-β induction.

484 While our scRNA-seq data did not reveal any correlations between viral genes
485 and IFN-β expression (6), technical limitations of short read sequencing may have
486 missed some important components. For example, the scRNA-seq would not have
487 captured mutations in KSHV that may have risen in individual cells. Moreover, the
488 sequencing method was 3' end directed, and many mRNAs in KSHV share 3' end
489 sequences, preventing accurate measurement of some viral genes. KSHV has evolved
490 a large arsenal of proteins that antagonize IFN signaling. KSHV ORF52 can prevent
491 cGAS activation by sequestering DNA substrates by phase separation mechanism (67),
492 and a truncated and therefore cytoplasmic form of KSHV LANA also inhibits cGAS (68).
493 KSHV ORF33 aids in inactivating the cGAS-adaptor STING (69). One study found that
494 the KSHV homolog of human IRFs vIRF1 inhibits IFN-β by preventing STING and TBK1
495 activation during KSHV reactivation in iSLK.219 cells (70). However, these viral factors
496 all act upstream of IRF3 activation, which is still active even in IFN-β-low cells in our
497 system, and are therefore unlikely to explain IFN induction heterogeneity. KSHV vIRFs
498 have also been implicated in regulating IFNs at the transcriptional level. Studies on
499 KSHV vIRF3 and vIRF4 have found that these inhibit IRF7, which is important for
500 inducing secondary responder cells (71, 72). A study on KSHV vIRF2 found that it
501 induces IRF3 degradation via caspase-3 (73). Another study found KSHV vIRF1 inhibits
502 IFNA4 induced by Newcastle Disease Virus in murine cells by preventing p300 from
503 binding to IRF1 and IRF3 (74). KSHV vIRF1 also binds CBP/p300 to prevent IRF3

504 complex formation on the IFN-β promoter during Sendai Virus infection in 293T cells
505 (75). Potentially, these events could create a barrier downstream of IRF3
506 phosphorylation, but this remains to be tested. Also, there has been no reports of any
507 KSHV factor that regulates AP-1 levels or blocks NF-κB activation, so there is no
508 obvious viral explanation for the heterogeneity we observe for these factors.

509 There are some limitations to our study. First, our reporter system likely does not
510 fully recapitulate native IFN-β mRNA expression and kinetics. The minimal IFN-β
511 promoter lacks the native chromatin environment and potential long range promoter
512 elements. The reporter also lacks the native 3' untranslated region of the IFN-β mRNA,
513 which makes this mRNA unstable. Also, it is likely that only cells with sustained IFN-β
514 promoter activity were detected and sorted, as sufficient accumulation of the tdTomato
515 protein is needed for FACS. However, despite these imperfections, we were able to
516 successfully separate the cells that expressed high and low levels of IFN-β at the time
517 of sorting (Fig. 1D). Also, while our results point to cellular heterogeneity as a major
518 determinant of IFN-β regulation, we cannot completely rule out the possibility that the
519 heterogeneity of AP-1 and NF-κB is regulated by the virus, as described above. Lastly,
520 while TPA is a very effective inducer of lytic KSHV reactivation and is commonly used in
521 KSHV research (35), it is also a known inducer of NF-κB. This is a potentially
522 confounding variable. Our concerns are reduced by the fact that treatments that induce
523 IFN-β in infected BC-3 cells do not induce IFN-β or phosphorylation of TBK1, IRF3, or
524 RelA in the uninfected BJAB cells at comparable time points, indicating viral reactivation
525 rather than TPA treatment drives signaling changes in our system (Figs. 1I, 4I, 5K).
526 Moreover, to date, all our results are consistent between the BC-3 and iSLK.219 KSHV-

527 infected cell lines, even though iSLK.219 cells are not treated with TPA to induce the
528 lytic cycle. This also suggests that our results are not simply due to TPA effects.
529 Despite the described limitations, this study points to a new model of
530 heterogeneous type I interferon transcription during viral infection as the result of
531 inherent cellular heterogeneity in protein levels and protein activation. More studies are
532 needed to pinpoint the earliest source of the heterogeneity and to examine the
533 mechanism of enrichment and activation of AP-1 and NF-κB in the context of antiviral
534 responses.
535
536 **Materials and Methods**
537
538 *Cell lines, reagents, and treatments*
539 All cells were cultured at 37°C and 5% CO_2. HEK293T cells were grown in Dulbecco's
540 modified Eagle's medium (DMEM; Life Technologies) supplemented with 10% fetal
541 bovine serum (FBS; Hyclone). BC-3 cells and derivatives were maintained at a density
542 of $5x10^5$ cells/mL in Roswell Park Memorial Institute medium (RPMI; Life Technologies)
543 supplemented with 20% FBS, 2 mM GlutaMAX (Gibco), and 55 μM β-mercaptoethanol
544 (BME; Gibco). BC-3-IFN-βp-tdTomato cells were generated as described in Lent,
545 Tabtieng, et al., 2022 (6). The transduced cells were purposefully not clonally selected,
546 because KSHV reactivation can be variable among KSHV-infected cells in a population
547 and clonal selection can result in artifacts. For reactivation, BC-3 and BC-3-IFN-βp-
548 tdTomato cells were seeded at a density of $5x10^5$ cells/mL and treated with 20 ng/mL
549 TPA (12-O-tetradecanoylphorbol-13-acetate; MilliporeSigma 5244001MG) in

550 dimethylsulfoxide (DMSO; Sigma Aldrich Fine Chemicals Biosciences). Where
551 indicated, cells were treated with vehicle (DMSO), 10 μM IDN-6556 (Emricasan; Selleck
552 Chemical LLC S777525MG), a mixture of neutralizing antibodies against type I IFNs at
553 1:2000 dilution (PBL Assay Science 39000-1), 10 μM TBK1 inhibitor (MRT67307;
554 Medchemexpress LLC HY130185MG), and/or 10 μM cGAS inhibitor (G140; Invivogen
555 inh-g140).
556
557 *Fluorescence-activated cell sorting*
558 100 mL of BC-3-IFN-βp-tdTomato cells were seeded at a density of $5x10^5$ cells/mL and
559 treated with TPA, IDN-1665, and, where indicated, an anti-IFN antibody mixture as
560 described above. After two days, they were collected and stained with 1 μg/mL DAPI
561 (4',6-Diamidino-2-Phenylindole, Dihydrochloride) stain (Invitrogen, D1306) for 5 minutes
562 at room temperature. They were then washed in phosphate buffer saline (PBS; Life
563 Technologies) and filtered through a 35 μm strainer (Chemglass Life Sciences
564 CLS4380009) and sorted based on tdTomato fluorescence on a BD FACSAria III at the
565 University of Wisconsin Carbone Cancer Center Flow Cytometry Laboratory core
566 facility. The DAPI stain was used to remove dead cells from the analysis, as in the
567 absence of permeabilization it only stains dead cells. Gates for tdTomato fluorescence
568 were drawn based on a negative control consisting of BC-3 cells that lack the reporter.
569 BC-3 cells lacking the reporter were treated in the same way as the sorted reporter
570 cells. In each experiment, about $80x10^6$ cells were sorted. $3x10^6$ tdTomato+ and $12x10^6$
571 tdTomato- cells were collected in each experiment. Sorted cells were pelleted and
572 resuspended in 1 mL of PBS. 100 μL of cell suspension were used for RNA extraction

573 and 900 μL for protein extraction. Bulk controls were prepared in parallel using 4 mL of
574 BC-3-IFN-βp-tdTomato cells seeded at a density of $5x10^5$ cells/mL and treated with
575 TPA, IDN-6556, anti-IFN antibodies, TBK1, or cGAS inhibitors (or corresponding
576 vehicle) as indicated for 2 days. The bulk control cells were pelleted and resuspended in
577 1 mL of PBS. 50 μL of cell suspension were used for RNA extraction, 450 μL for protein
578 extraction, and 500 μL for flow cytometry to determine KSHV reactivation efficiency.
579
580 *RT-qPCR*
581 RNA samples were collected from BC-3 or BC-3-IFN-βp-tdTomato cells reactivated for
582 2 days as described above or treated with vehicle. For experiments involving sorting, a
583 fraction of the sorted cells was used as described in the Fluorescence-activated cell
584 sorting section. For experiments not involving sorting, 4 mL of BC-3/ BC-3-IFN-βp-
585 tdTomato cells were collected as described in the same section for bulk control
586 samples. In both cases, cells to be lysed were pelleted by centrifugation and
587 resuspended in RNA lysis buffer (Zymo research). Total RNA was extracted using the
588 Quick-RNA MiniPrep kit (Zymo research) following the manufacturer's protocol. cDNA
589 was prepared using an iScript cDNA synthesis kit (Bio-Rad) following the
590 manufacturer's protocol. Real-time quantitative PCR (RT-qPCR) was performed using
591 iTaq Universal SYBR green Supermix (Bio-Rad) following the manufacturer's protocol in
592 CFX Duet Real-Time PCR System (Bio-Rad). For KSHV gene ORF50, cDNA was
593 prepared using AMV RT (Promega) following the manufacturer's protocol using 1 pmol
594 reverse primer for ORF50 to select for transcripts from the correct strand of the
595 genome. No-template and no-RT controls were included in each replicate experiment,

596 and experiments were only included if these controls showed negligible amplification
597 rates. In all cases, target mRNA levels were normalized to levels of 18S rRNA as an
598 internal standard. CFX Maestro software was used to analyze the data. Primers specific
599 for each gene:

Target	Forward 5' → 3'	Reverse 5' → 3'	ref
Human IFN-β	GTCAGAGTGGAAATCCTAAG	ACAGCATCTGCTGGTTGAAG	(76)
Human 18S rRNA	GTAACCCGTTGAACCCCATT	CCATCCAATCGGTAGTAGCG	(77)
Human MxA	ATCCTGGGATTTTGGGGCTT	CCGCTTGTCGCTGGTGTCG	(78)
tdTomato	ACATCCCCGATTACAAGAAGC	TTGTAGATCAGCGTGCCGTC	(79)
Human IFN-λ1	CGCCTTGGAAGAGTCACTCA	GAAGCCTCAGGTCCCAATTC	(80)
KSHV ORF50	ACCAAGGTGTGCCGTGTAGAGATT	AGCCTTACGCTTCTTTGAGCTCCT	(81)

600

601 *Protein analysis*

602 Protein samples were collected from BC-3/BC-3-IFN-βp-tdTomato cells reactivated for 2
603 days as described above or treated with vehicle. For experiments involving sorting, a
604 fraction of the sorted cells was used as described in the Fluorescence-activated cell
605 sorting section. For samples not involving in sorting, 4 mL of BC-3/ BC-3-IFN-βp-
606 tdTomato cells were used and collected as described for bulk control samples in that
607 section. In both cases, cells to be lysed were pelleted by centrifugation and
608 resuspended in an NP-40-only buffer (50 mM Tris-HCl pH 7.4, 150 mM NaCl, 1 mM
609 EDTA, 0.5% NP-40) supplemented with a broad-spectrum protease inhibitor mixture
610 (Thermo Scientific A32955) and a broad-spectrum phosphatase inhibitor mixture
611 (Thermo Scientific A32957). Protein concentration was determined by Bradford method
612 (Bio-Rad 5000006). Between 10 and 20 µg of protein were loaded on each gel. Laemmli
613 buffer (Bio-Rad) was added to samples before incubation at 95°C for 5 min. Samples
614 were separated by SDS-PAGE and transferred to polyvinylidene difluoride membranes
615 (PVDF; Fisher Scientific IPFL00010) using the semi-dry Trans-Blot Turbo Transfer

616 System (Bio-Rad). Membranes were blocked in 5% bovine serum albumin (BSA; Fisher
617 BioReagents BP1600-100) in Tris-Buffer Saline with 0.1% Tween (TBST). All antibodies
618 used were diluted 1:1000 in 5% BSA in TBST for staining. The following Cell Signaling
619 Technologies antibodies were used: IRF3 (D6I4C, no.11904), phospho-IRF3 Ser386
620 (E7J8G, no.37829), TBK1 (D1B4, no.3504), phospho-TBK1 Ser172 (D52C2, no.5483),
621 ATF2 (D4L2X, no.35031), c-Jun (60A8, no.9165), NF-κB p65/RelA (D14E12, no.8242),
622 phospho-NF-κB p65/RelA Ser536 (93H1, no.3303). In addition, antibodies against β-
623 actin (Abcam, ab8229) were used to stain for loading controls. Secondary horseradish
624 peroxidase (HRP)-conjugated antibodies (goat anti-rabbit and rabbit anti-goat IgG) were
625 purchased from Southern Biotechnology (no.4030-05, no.OB6106-05) and used at
626 1:5000 in 5% BSA in TBST. All membranes were exposed using SuperSignal West Pico
627 PLUS Chemiluminescent Substrate (Thermo Scientific) and imaged with an iBright
628 FL1000 imaging system (Thermo Scientific). Protein quantification from western images
629 was done using Image J (82).
630
631 *Flow cytometry analysis*
632 BC-3-IFN-βp-tdTomato cells were fixed with 4% paraformaldehyde (PFA; Electron
633 Microscopy Sciences) in PBS for 15 min at room temperature and washed twice with
634 PBS. Then, the cells were permeabilized by incubating in ice cold 90% methanol diluted
635 in 0.5% BSA in PBS for 5 min on ice and washed twice with 0.5% BSA in PBS. For
636 assessment of reactivation efficiency, cells were stained for a KSHV lytic infection
637 marker, ORF45. They were incubated with antibodies against KSHV ORF45 (Thermo
638 Fisher MA514769) at 1:100 dilution for 1 hr at room temperature, washed twice, and

639 then stained with Alexa Fluor 647 (AF647)-conjugated secondary antibody at 1:500
640 dilution (Thermo Fisher A21236) for 30 min at room temperature in the dark. 0.5 % BSA
641 in PBS was used for all incubations and washes. Cells were collected by centrifugation
642 at 500 x *g* for 5 min between all washes/incubation. After two washes, cells were
643 resuspended in 0.5% BSA in PBS and filtered through a 35 µm strainer (Chemglass Life
644 Sciences CLS4380009) for analysis. Fluorescence was quantified by flow cytometry on
645 a Thermo Fisher Attune NxT V6 cytometer at the UW-Madison Carbone Cancer Center
646 Flow Cytometry Laboratory. AF647 fluorescence was gated based on the corresponding
647 latently infected and vehicle (DMSO)-treated cells. $3x10^6$ events were collected per
648 sample. FlowJo 10.8.2 was used for the data analysis.
649
650 *Single cell RNA sequencing analysis*
651 A dataset obtained from iSLK.219 cell samples previously published in Lent, Tabtieng,
652 et al., 2022 (6) (GSE190558) was re-analyzed in the current study by extracting
653 prepared Seurat matrices and manually selecting genes of interest.
654
655 *Statistics*
656 All statistical analysis was performed using GraphPad Prism version 10.3.0 or later
657 (GraphPad Software, Boston, MA USA; www.graphpad.com). Statistical significance
658 was determined by One- or Two-way ANOVA followed by a *post hoc* multiple-
659 comparison test (Dunnett or Tukey) when multiple comparisons were required.
660 Statistical analysis of qRT-PCR data was performed on log_2 transformed data to ensure
661 normal distribution (83). Singular outliers were identified using Grubbs' test (alpha =

662 0.05) for outliers, and removed from Fig. 1I-J, Fig. 2A, and Fig. 3D, F, G. All plots
663 represent mean +/- standard deviation. Figure legends indicate the number of biological
664 replicates used for each experiment. All western blot images are representative of 3 or
665 more independent biological replicates.
666

667 **Acknowledgements**

668 We thank members of the Gaglia laboratory for suggestions and feedback on the
669 project and the manuscript. We thank the University of Wisconsin Carbone Cancer
670 Center (UWCCC) Flow Cytometry Laboratory staff for technical and conceptual
671 assistance and services. This work was supported by National Institutes of Health Grant
672 R01 CA268976 to M.M.G. and by the University of Wisconsin-Madison, Office of the
673 Vice Chancellor for Research and Graduate Education with funding from the Wisconsin
674 Alumni Research Foundation. The UWCCC Flow Cytometry Laboratory is supported by
675 the UWCCC Cancer Center Grant P30 CA014520.

676 **References**

677 1. Schoggins JW, Wilson SJ, Panis M, Murphy MY, Jones CT, Bieniasz P, Rice CM. 2011.
678 A diverse array of gene products are effectors of the type I interferon antiviral response.
679 Nature 472.
680 2. Schoggins JW, Rice CM. 2011. Interferon-stimulated genes and their antiviral effector
681 functions. Curr Opin Virol 1:7.
682 3. Taft J, Bogunovic D. 2018. The Goldilocks Zone of Type I IFNs: Lessons from Human
683 Genetics. J Immunol 201:7.
684 4. González-Navajas JM, Lee J, David M, Raz E. 2012. Immunomodulatory functions of
685 type I interferons. Nat Rev Immunol 12:11.
686 5. Kobayashi KS, Flavell RA. 2004. Shielding the double-edged sword: negative regulation
687 of the innate immune system. J Leukoc Biol 75:6.
688 6. Tabtieng T, Lent RC, Kaku M, Monago Sanchez A, Gaglia MM. 2022. Caspase-
689 Mediated Regulation and Cellular Heterogeneity of the cGAS/STING Pathway in
690 Kaposi's Sarcoma-Associated Herpesvirus Infection. mBio e0244622.
691 7. Hamele CE, Russell AB, Heaton NS. 2022. In Vivo Profiling of Individual Multiciliated
692 Cells during Acute Influenza A Virus Infection. J Virol 96.
693 8. Hein MY, Weissman JS. 2022. Functional single-cell genomics of human
694 cytomegalovirus infection. Nat Biotechnol 40:11.
695 9. Fiege JK, Thiede JM, Nanda HA, Matchett WE, Moore PJ, Montanari NR, Thielen BK,
696 Daniel J, Stanley E, Hunter RC, Menachery VD, Shen SS, Bold TD, Langlois RA. 2021.
697 Single cell resolution of SARS-CoV-2 tropism, antiviral responses, and susceptibility to
698 therapies in primary human airway epithelium. PLoS Pathog 17.
699 10. Sun J, Vera JC, Drnevich J, Lin YT, Ke R, Brooke CB. 2020. Single cell heterogeneity in
700 influenza A virus gene expression shapes the innate antiviral response to infection.
701 PLoS Pathog 16.
702 11. Russell AB, Elshina E, Kowalsky JR, Te Velthius AJW, Bloom JD. 2019. Single-Cell
703 Virus Sequencing of Influenza Infections That Trigger Innate Immunity. J Virol 93.
704 12. Drayman N, Patel P, Vistain L, Tay S. 2019. HSV-1 single-cell analysis reveals the
705 activation of anti-viral and developmental programs in distinct sub-populations. Elife 8.
706 13. O'Neal JT, Upadhyay A, Wolabaugh A, Patel NB, Bosinger SE, Suthar MS. 2019. West
707 Nile Virus-Inclusive Single-Cell RNA Sequencing Reveals Heterogeneity in the Type I
708 Interferon Response within Single Cells. J Virol 93.
709 14. Russell AB, Trapnell C, Bloom JD. 2018. Extreme heterogeneity of influenza virus
710 infection in single cells. Elife 7.
711 15. Killip MJ, Jackson R, Pérez-Cidoncha M, Fodor E, Randall RE. 2017. Single-cell studies
712 of IFN-β promoter activation by wild-type and NS1-defective influenza A viruses. J Gen
713 Virol 98:7.
714 16. Pérez-Cidoncha M, Killip MJ, Oliveros JC, Asensio VJ, Fernández Y, Bengoechea JA,
715 Randall RE, Ortín J. 2014. An unbiased genetic screen reveals the polygenic nature of
716 the influenza virus anti-interferon response. J Virol 88:15.
717 17. Kallfass C, Lienenklaus S, Weiss S, Staeheli P. 2013. Visualizing the beta interferon
718 response in mice during infection with influenza A viruses expressing or lacking
719 nonstructural protein 1. J Virol 87:6.
720 18. Hu J, Nudelman G, Shimoni Y, Kumar M, Ding Y, López C, Hayot F, Wetmur JG,
721 Sealfon S. 2011. Role of cell-to-cell variability in activating a positive feedback antiviral
722 response in human dendritic cells. PLoS One 6.
723 19. Hu J, Sealfon S, Hayot F, Jayaprakash C, Kumar M, Pendleton AC, Ganee A,
724 Fernandez-Sesma A, Moran TM, Wetmur JG. 2007. Chromosome-specific and noisy

IFNB1 transcription in individual virus-infected human primary dendritic cells. Nucleic Acids Res 35:10.

20. Tabtieng T, Degterev A, Gaglia MM. 2018. Caspase-Dependent Suppression of Type I Interferon Signaling Promotes Kaposi's Sarcoma-Associated Herpesvirus Lytic Replication. J Virol 92.

21. Zhao M, Zhang J, Phatnani H, Scheu S, Maniatis T. 2012. Stochastic expression of the interferon-β gene. PLoS Biol 10.

22. Rand U, Rinas M, Schwerk J, Nöhren G, Linnes M, Kröger A, Flossdorf M, Kály-Kullai K, Hauser H, Höfer T, Köster M. 2012. Multi-layered stochasticity and paracrine signal propagation shape the type-I interferon response. Mol Syst Biol 8.

23. Panne D, Maniatis T, Harrison SC. 2007. An atomic model of the interferon-beta enhanceosome. Cell 129:13.

24. Maniatis T, Falvo JV, Kim TH, Kim TK, Lin CH, Parekh BS, Wathelet MG. 1998. Structure and function of the interferon-beta enhanceosome. Cold Spring Harb Symp Quant Biol 63:12.

25. Apostolou E, Thanos D. 2008. Virus Infection Induces NF-kappaB-dependent interchromosomal associations mediating monoallelic IFN-beta gene expression. Cell 134:7.

26. Arvanitakis L, Mesri EA, Nador RG, Said JW, Asch AS, Knowles DM, Cesarman E. 1996. Establishment and characterization of a primary effusion (body cavity-based) lymphoma cell line (BC-3) harboring kaposi's sarcoma-associated herpesvirus (KSHV/HHV-8) in the absence of Epstein-Barr virus. Blood 88.

27. Li K, Chen Z, Kato N, Gale K, Lemon SM. 2005. Distinct poly(I-C) and virus-activated signaling pathways leading to interferon-beta production in hepatocytes. J Biol Chem 280:9.

28. Guo F, Mead J, Aliya N, Wang L, Cuconati A, Wei L, Li K, Block TM, Guo JT, Chang J. 2012. RO 90-7501 enhances TLR3 and RLR agonist induced antiviral response. PLoS One 7.

29. Gentili M, Kowal J, Tkach M, Satoh T, Lahaye X, Conrad C, Boyron M, Lombard B, Durand S, Kroemer G, Loew D, Dalod M, Thery C, Manel N. 2015. Transmission of innate immune signaling by packaging of cGAMP in viral particles. Science 349.

30. Day RN, Davidson MW. 2009. The fluorescent protein palette: tools for cellular imaging. Chem Soc Rev 38:34.

31. Muzumdar MD, Tasic B, Miyamichi K, Li L, Luo L. 2007. A global double-fluorescent Cre reporter mouse. Genesis 45:13.

32. Surre J, Saint-Ruf C, Collin V, Orenga S, Ramjeet M, Matic I. 2018. Strong increase in the autofluorescence of cells signals struggle for survival. Sci Rep 8.

33. Chance B, Schoener B, Oshino R, F. I, Nakase Y. 1979. Oxidation-reduction ratio studies of mitochondria in freeze-trapped samples. NADH and flavoprotein fluorescence signals. J Biol Chem 254:8.

34. Brulois KF, Chang H, Lee ASY, Ensser A, Wong LY, Toth Z, Lee SH, Lee HR, Myoung J, Ganem D, Oh TK, Kim JF, Gao SJ, Jung JU. 2012. Construction and Manipulation of a New Kaposi's Sarcoma-Associated Herpesvirus Bacterial Artificial Chromosome Clone. J Virol 86.

35. Cohen A, Brodie C, Sarid R. 2006. An essential role of ERK signalling in TPA-induced reactivation of Kaposi's sarcoma-associated herpesvirus. J Gen Virol 87:8.

36. Renne R, Zhong W, Herndier B, McGrath M, Abbey N, Kedes D, Ganem D. 1996. Lytic growth of Kaposi's sarcoma-associated herpesvirus (human herpesvirus 8) in culture. Nat Med 2:5.

37. Kikkawa U, Matsuzaki H, Yamamoto T. 2002. Protein kinase C delta (PKC delta): activation mechanisms and functions. J Biochem 132:9.

38. Duquesnes N, Lezoualc'h F, Crozatier B. 2011. PKC-delta and PKC-epsilon: foes of the same family or strangers? J Mol Cell Cardiol 51:9.
39. Menezes J, Leibold W, Klein G, Clemens G. 1975. Establishment and characterization of an Epstein-Barr virus (EBC)-negative lymphoblastoid B cell line (BJA-B) from an exceptional, EBV-genome-negative African Burkitt's lymphoma. Biomedicine 22:9.
40. Sun Z, Xiao B, Jha HC, Lu J, Banerjee S, Robertson ES. 2014. Kaposi's sarcoma-associated herpesvirus-encoded LANA can induce chromosomal instability through targeted degradation of the mitotic checkpoint kinase Bub1. J Virol 88:11.
41. Domsic JF, Chen HS, Lu F, Marmorstein R, Lieberman PM. 2013. Molecular basis for oligomeric-DNA binding and episome maintenance by KSHV LANA. PLoS Pathog 9.
42. Ma F, Li B, Liu S, Iyer SS, Yu Y, Wu A, Cheng G. 2015. Positive feedback regulation of type I IFN production by the IFN-inducible DNA sensor cGAS. 194 4:10.
43. Onoguchi K, Yoneyama M, Takemura A, Akira S, Taniguchi T, Namiki H, Fujita T. 2007. Viral infections activate types I and III interferon genes through a common mechanism. J Biol Chem 282:6.
44. Osterlund PI, Pietilä TE, Veckman V, Kotenko SV, Julkunen I. 2007. IFN regulatory factor family members differentially regulate the expression of type III IFN (IFN-lambda) genes. Immunity 179:9.
45. Lenardo MJ, Fan CM, Maniatis T, Baltimore D. 1989. The involvement of NF-kappa B in beta-interferon gene regulation reveals its role as widely inducible mediator of signal transduction. Cell 57:8.
46. Wathelet MG, Lin CH, Parekh BS, Ronco LV, Howley PM, Maniatis T. 1998. Virus infection induces the assembly of coordinately activated transcription factors on the IFN-beta enhancer in vivo. Mol Cell 1:11.
47. Iversen MB, Paludan SR. 2010. Mechanisms of type III interferon expression. J Interferon Cytokine Res 30:6.
48. Holländer GA. 1999. On the stochastic regulation of interleukin-2 transcription. Semin Immunol 11:11.
49. Guo L, Hu-Li J, Paul WE. 2004. Probabilistic regulation of IL-4 production in Th2 cells: accessibility at the Il4 locus. Immunity 20:11.
50. Guo L, Hu-Li J, Paul WE. 2005. Probabilistic regulation of IL-4 production. J Clin Immunol 25:9.
51. Kelly BL, Locksley RM. 2000. Coordinate regulation of the IL-4, IL-13, and IL-5 cytokine cluster in Th2 clones revealed by allelic expression patterns. J Immunol 165:5.
52. Calado DP, Paixão T, Holmberg D, Haury M. 2006. Stochastic monoallelic expression of IL-10 in T cells. J Immunol 177:7.
53. Ishikawa H, Barber GN. 2008. STING is an endoplasmic reticulum adaptor that facilitates innate immune signalling. Nature 455:5.
54. Balka KR, Louis C, Saunders TL, Smith AM, Calleja DJ, D'Silva DB, Moghaddas F, Tailler M, Lawlor KE, Zhan Y, Burns CJ, Wicks IP, Miner JJ, Kile BT, Masters SL, De Nardo D. 2020. TBK1 and IKKε Act Redundantly to Mediate STING-Induced NF-κB Responses in Myeloid Cells. Cell Rep 31.
55. Sakurai H, Chiba H, Miyoshi H, Sugita T, Toriumi W. 1999. IkappaB kinases phosphorylate NF-kappaB p65 subunit on serine 536 in the transactivation domain. J Biol Chem 274:4.
56. Mattioli I, Sebald A, Bucher C, Charles RP, Nakano H, Doi T, Kracht M, Schmitz ML. 2004. Transient and selective NF-kappa B p65 serine 536 phosphorylation induced by T cell costimulation is mediated by I kappa B kinase beta and controls the kinetics of p65 nuclear import. J Immunol 172:9.
57. Buss H, Dörrie A, Schmitz ML, Hoffmann E, Resch K, Kracht M. 2004. Constitutive and interleukin-1-inducible phosphorylation of p65 NF-{kappa}B at serine 536 is mediated by

827 multiple protein kinases including I{kappa}B kinase (IKK)-{alpha}, IKK{beta},
828 IKK{epsilon}, TRAF family member-associated (TANK)-binding kinase 1 (TBK1), and an
829 unknown kinase and couples p65 to TATA-binding protein-associated factor II31-
830 mediated interleukin-8 transcription. J Biol Chem 279:10.
831 58. Sakurai H, Miyoshi H, Toriumi W, Sugita T. 1999. Functional interactions of transforming
832 growth factor beta-activated kinase 1 with IkappaB kinases to stimulate NF-kappaB
833 activation. J Biol Chem 274:8.
834 59. Parekh N, Winship D, Dis EV, Stetson DB. 2024. Regulation and Dynamics of IFN-β
835 Expression Revealed with a Knockin Reporter Mouse. J Immunol 213:11.
836 60. Shalek AK, Satija R, Shuga J, Trombetta JJ, Gennert D, Lu D, Chen P, Gertner RS,
837 Gaublomme JT, Yosef N, Schwartz S, Fowler B, Weaver S, Wang J, Wang X, Ding R,
838 Raychowdhury R, Friedman N, Hacohen N, Park H, May AP, Regev A. 2014. Single-cell
839 RNA-seq reveals dynamic paracrine control of cellular variation. Nature 510:7.
840 61. Strahle L, Garcin D, Kolakofsky D. 2006. Sendai virus defective-interfering genomes and
841 the activation of interferon-beta. Virology 351:11.
842 62. Johnston MD. 1981. The characteristics required for a Sendai virus preparation to
843 induce high levels of interferon in human lymphoblastoid cells. J Gen Virol 56:10.
844 63. Patil S, Fribourg M, Ge Y, Batish M, Tyagi S, Hayot F, Sealfon S. 2015. Single-cell
845 analysis shows that paracrine signaling by first responder cells shapes the interferon-β
846 response to viral infection. Sci Signal 8.
847 64. Hwang SY, Hur KY, Kim JR, Cho KH, Kim SH, Yoo JY. 2013. Biphasic RLR-IFN-β
848 response controls the balance between antiviral immunity and cell damage. J Immunol
849 190:9.
850 65. Zawatzky R, Maeyer ED, Maeyer-Guignard JD. 1985. Identification of individual
851 interferon-producing cells by in situ hybridization. PNAS 82:5.
852 66. Enoch T, Zinn K, Maniatis T. 1986. Activation of the human beta-interferon gene
853 requires an interferon-inducible factor. Mol Cell Biol 6:10.
854 67. Bhowmik D, Tian Y, Wang B, Zhu F, Yin Q. 2022. Structural basis of higher order
855 oligomerization of KSHV inhibitor of cGAS. PNAS 199.
856 68. Zhang G, Chan B, Samarina N, Abere B, Weidner-Glunde M, Buch A, Pich A,
857 Brinkmann MM, Schulz TF. 2016. Cytoplasmic isoforms of Kaposi sarcoma herpesvirus
858 LANA recruit and antagonize the innate immune DNA sensor cGAS. PNAS 133.
859 69. Yu K, Tian H, Deng H. 2020. PPM1G restricts innate immune signaling mediated by
860 STING and MAVS and is hijacked by KSHV for immune evasion. Sci Adv 6.
861 70. Ma Z, Jacobs SR, West JA, Stopford C, Zhang Z, Davis Z, Barber GN, Glausinger BA,
862 Dittmer DP, Damania B. 2015. Modulation of the cGAS-STING DNA sensing pathway by
863 gammaherpesviruses. PNAS 112.
864 71. Joo CH, Shin YC, Gack M, Wu L, Levy D, Jung JU. 2007. Inhibition of Interferon
865 Regulatory Factor 7 (IRF7)-Mediated Interferon Signal Transduction by the Kaposi's
866 Sarcoma-Associated Herpesvirus Viral IRF Homolog vIRF3. J Virol 81:10.
867 72. Hwang SW, Kim D, Jung JU, Lee HR. 2017. KSHV-encoded viral interferon regulatory
868 factor 4 (vIRF4) interacts with IRF7 and inhibits interferon alpha production. Biochem
869 Biophys Res Commun 486:6.
870 73. Aresté C, Mutocheluh M, Blackbourn DJ. 2009. Identification of caspase-mediated decay
871 of interferon regulatory factor-3, exploited by a Kaposi sarcoma-associated herpesvirus
872 immunoregulatory protein. J Biol Chem 284:13.
873 74. Burysek L, Yeow WS, Lubyova B, Kellum M, Schafer SL, Huang YQ, Pitha PM. 1999.
874 Functional Analysis of Human Herpesvirus 8-Encoded Viral Interferon Regulatory Factor
875 1 and Its Association with Cellular Interferon Regulatory Factors and p300. J Virol 73.

876 75. Lin R, Genin P, Mamane Y, Sgarbanti M, Battistini A, Harrington WJ, Barber GN, Hiscott
877 J. 2001. HHV-8 encoded vIRF-1 represses the interferon antiviral response by blocking
878 IRF-3 recruitment of the CBP/p300 coactivators. Oncogene 20:12.
879 76. Yang Q, Elz AE, Panis M, Liu T, Nilsson-Payant BE, Blanco-Melo D. 2023. Modulation of
880 Influenza A virus NS1 expression reveals prioritization of host response antagonism at
881 single-cell resolution. Front Microbiol 14.
882 77. Schmittgen TD, Zakrajsek BA. 2000. Effect of experimental treatment on housekeeping
883 gene expression: validation by real-time, quantitative RT-PCR. J Biochem Biophys
884 Methods 46:11.
885 78. Zhu FX, Sathish N, Yuan Y. 2010. Antagonism of host antiviral responses by Kaposi's
886 sarcoma-associated herpesvirus tegument protein ORF45. PLoS One 5.
887 79. Valny M, Honsa P, Waloschkova E, Matuskova H, Kriska J, Kirdajova D, Androvic P,
888 Valihrach L, Kubista M, Anderova M. 2018. A single-cell analysis reveals multiple roles
889 of oligodendroglial lineage cells during post-ischemic regeneration. Glia 66:14.
890 80. Ank N, West H, Bartholdy C, Eriksson K, Thomsen AR, Paludan S. 2006. Lambda
891 interferon (IFN-lambda), a type III IFN, is induced by viruses and IFNs and displays
892 potent antiviral activity against select virus infections in vivo. J Virol 80:9.
893 81. Rossetto CC, Pari G. 2012. KSHV PAN RNA associates with demethylases UTX and
894 JMJD3 to activate lytic replication through a physical interaction with the virus genome.
895 PLoS Pathog 8.
896 82. Stael S, Miller LP, Fernández-Fernández ÁD, Van Breusegem F. 2022. Detection of
897 Damage-Activated Metacaspase Activity by Western Blot in Plants. Methods Mol Biol
898 2447:11.
899 83. Edmunds RC, McIntyre JK, Luckenbach JA, Baldwin DH, Incardona JP. 2014. Toward
900 Enhanced MIQE Compliance: Reference Residual Normalization of qPCR Gene
901 Expression Data. J Biomol Tech 25:7.
902

903 **Figure Legends**

904

905 **Figure 1. An IFN-β-promoter driven fluorescent reporter allows isolation of cells**
906 **expressing high and low levels of IFN-β. A.** Diagram of the IFN-βp-tdTomato reporter
907 and sorting strategy. Two copies of the 303 bp minimal promoter sequence for the
908 human IFNB1 gene were cloned in front of the tdTomato fluorophore. This cassette was
909 then introduced in BC-3 cells via lentiviral transduction for stable integration. Cells were
910 sorted based on tdTomato expression and RNA and protein samples were collected
911 from the same experiment. **B-H.** BC3-IFN-βp-tdTomato reporter cells were treated with
912 20 ng/mL TPA for 48 hours to induce the lytic cycle ("lytic (+TPA)"). Where indicated,
913 the cells were also treated with 10 μM of the pan-caspase inhibitor IDN-6556 ("casp-i").
914 **B.** Gating strategy for FACS. **C-E, G-H.** IFN-β, tdTomato, and ORF50 mRNA levels
915 were measured by RT-qPCR and normalized to 18S rRNA. For **C-E** and **H**, mRNA
916 levels are plotted relative to the lytic+casp-i sample. For **G,** mRNA levels are plotted
917 relative to the lytic sample. **H.** Cells were stained for KSHV ORF45 and analyzed by
918 flow cytometry. **I-J.** KSHV-negative BJAB cells were treated with 20 ng/mL TPA for 48
919 hours. Where indicated, the cells were also treated with 10 μM of the pan-caspase
920 inhibitor IDN-6556 ("casp-i"). BC3 cells treated with 20 ng/mL TPA and 10 μM of the
921 pan-caspase inhibitor IDN-6556 ("casp-i") were used as a positive control. IFN-β and
922 IFN- λ1 mRNA levels were measured by RT-qPCR and normalized to 18S rRNA. They
923 are plotted relative to the BC3 positive control. ns = $p>0.05$, ** = $p<0.01$, *** = $p<0.001$,
924 **** = $p<0.0001$. One-Way ANOVA followed by Dunnett's (C, F, G, I, J) or Tukey's (D,
925 E, H) post hoc multiple comparisons test. $n \geq 4$ for all experiments.

926

927 **Figure 2. The IFN-β reporter allows isolation of cells expressing high and low**
928 **levels of IFN-β when paracrine signaling is blocked.** BC3-IFN-βp-tdTomato reporter
929 cells were treated with 20 ng/mL TPA for 48 hours to induce the lytic cycle ("lytic
930 (+TPA)"). Where indicated, the cells were also treated with 10 μM of the pan-caspase
931 inhibitor IDN-6556 ("casp-i") and a cocktail of antibodies against type I IFNs and their
932 receptor ("anti-IFN Abs") at 1:2000 dilution. **A-C, E-F.** IFN-β, tdTomato, and ORF50
933 mRNA levels were measured by RT-qPCR and normalized to 18S rRNA. For **A-C** and
934 **F**, mRNA levels are plotted relative to the lytic+casp-i sample. For **E**, mRNA levels are
935 plotted relative to the lytic sample. **D.** Cells were stained for KSHV ORF45 and analyzed
936 by flow cytometry. ns = $p>0.05$, ** = $p<0.01$, *** = $p<0.001$, **** = $p<0.0001$. One-Way
937 ANOVA followed by Dunnett's (A, D, E) or Tukey's (B, C, F) post hoc multiple
938 comparisons test. $n \geq 4$ for all experiments.

939

940 **Figure 3. IFN-λ1 and IFN-β are coordinately induced in a subset of cells, pointing**
941 **to heterogeneity in the induction pathway rather than stochastic noise in**
942 **expression. A.** Diagram of coordinate induction of IFN-β and IFN-λ. In "first responder"
943 cells, IFN-β and IFN-λ are induced in response to infection or lytic reactivation
944 downstream of PRRs. In "secondary responder" cells, ISGs such as MxA and many
945 components of the IFN induction pathway like IRF7 are induced in response to signaling
946 downstream of IFN receptors. Induction of genes like IRF7 potentiates IFN induction in
947 these cells. Anti-IFN antibodies block paracrine signaling from IFN-β to prevent ISG
948 induction and potentiation of IFN induction in secondary responder cells. **B-I.** BC3-IFN-

949 βp-tdTomato reporter cells were treated with 20 ng/ml TPA for 48 hours to induce the
950 lytic cycle ("lytic (+TPA)"). Where indicated, the cells were also treated with 10 μM of the
951 pan-caspase inhibitor IDN-6556 ("casp-i") and/or a cocktail of antibodies against type I
952 IFNs and their receptor ("anti-IFN Abs") at 1:2000 dilution. IFN-λ1 (**B-E**) and MxA (**F-I**)
953 mRNA levels were measured by RT-qPCR and normalized to 18S rRNA. In **B**-**D**, and **F-**
954 **H,** IFN-λ1 and MxA mRNA levels are plotted relative to the lytic+casp-i sample. In **E** and
955 **I,** IFN-λ1 and MxA mRNA levels are plotted relative to the lytic+casp-i+anti-IFN Abs
956 sample. The lytic+casp-i (**C, G**) or the lytic+casp-i+anti-IFN Abs (**E, I**) samples were
957 sorted based on tdTomato expression and the fold enrichment in IFN-λ1 (**C, E**) and MxA
958 (**G, I**) mRNA levels compared to unsorted ("bulk") samples are plotted in $\log_2$ scale.
959 Results in this figure were obtained from the same samples used in Fig. 1 and are thus
960 directly comparable to IFN-β enrichment shown in that Figure. ns = $p>0.05$, * = $p<0.05$,
961 ** = $p<0.01$, **** = $p<0.0001$, One-Way ANOVA followed by Dunnett's (B, D, F, H) or
962 Tukey's (C, E, G, I) post hoc multiple comparisons test. $n \geq 4$ for all experiments.
963

964 **Figure 4. TBK1 and IRF3 are necessary but not sufficient to direct IFN-β**
965 **expression, as they are activated even in cells with low IFN-β expression.** BC3-
966 IFN-βp-tdTomato reporter cells were treated with 20 ng/ml TPA for 48 hours to induce
967 the lytic cycle ("lytic (+TPA)"). Where indicated, the cells were also treated with 10 μM of
968 the pan-caspase inhibitor IDN-6556 ("casp-i"), 10 μM of the TBK1 inhibitor MRT76307
969 ("TBK1i"), 10 μM of the cGAS inhibitor G140 ("cGASi"), and/or a cocktail of antibodies
970 against type I IFNs and their receptor ("anti-IFN Abs") at 1:2000 dilution. **A-B.** IFN-β and
971 IFN-λ1 mRNA levels were measured by qRT-PCR and normalized to 18S rRNA. The

expression levels are plotted relative to “untreated” lytic+casp-i samples that did not receive TBK1i or cGASi treatment for each experiment. n=3. **** = p<0.0001. Two-Way ANOVA followed by Tukey’s post hoc multiple comparisons test. **B-H.** Protein lysates were probed for phosphorylated IRF3 (Ser386), total IRF3, phosphorylated TBK1 (Ser172), total TBK1, and β-actin as a loading control. As a positive control for IRF3 and TBK1 activation/phosphorylation, A549 cells were treated with poly(I:C) for 6 and 48 hours before protein lysates were collected. Protein was isolated from treated BC3-IFN-βp-tdTomato reporter cells without sorting (“bulk”), or after sorting the lytic+casp-i (**C-E**) or lytic+casp-i+anti-IFN Abs (**F-H**) sample based on tdTomato expression (**D-E, G-H)**. Western blot for phosphorylated TBK1 and phosphorylated IRF3 for bulk lytic+casp-i or lytic+casp-i+anti-IFN Abs treated samples and sorted tdTomato+ and tdTomato- samples were quantified by normalizing the density of phosphorylated protein to unphosphorylated protein bands. Phosphorylation levels are plotted relative to the bulk lytic+casp-i or lytic+casp-i+anti-IFN Abs treated samples. **I.** KSHV-negative BJAB cells were treated with vehicle, 20 ng/ml TPA, and/or 10 μM of the pan-caspase inhibitor IDN-6556 (“casp-i”) for 48 hours. Protein was isolated and stained for phosphorylated TBK1, total TBK1, phosphorylated IRF3, and total IRF3. Images shown are representative of 3 replicates (**A-H**) or 2 replicates (**I**).

Figure 5. Levels of the AP-1 subunit ATF2 and phosphorylation of the NF-κB subunit RelA are higher in cells with high IFN-β expression. A. Diagram of the IFN-β enhanceosome and its position on the IFN-β promoter. In the IFN-β enhanceosome, NF-κB is composed of subunits NFKB1 (p50) and RelA, and AP-1 is composed of

995 subunits ATF2 and c-Jun. **B-C.** Re-analysis of single-cell RNA sequencing (scRNA-seq)
996 data in Tabtieng, Lent, et al 2022. iSLK.219 cells were treated with 1 μg/mL doxycycline
997 for 4 days to induce the lytic cycle ("lytic"). The cells were also treated with 10 μM of the
998 pan-caspase inhibitor IDN-6556 ("casp-i"), as well as a mixture of antibodies against
999 type I IFNs and its receptor ("anti-IFN Abs") (**C** only) to block IFN-β paracrine signaling.
1000 The average mRNA levels of genes in the IFN-β enhanceosome from the scRNA-seq
1001 data are shown for each of the 12 clusters of cells identified by the original analysis
1002 (indicated by different colors above the heatmap). Clusters were classified as "latent".
1003 "lytic", or "lytic IFN-β-positive" based on the pattern of viral genes they expressed and
1004 whether they also expressed IFN-β. The "lytic IFN-β-positive" clusters were further
1005 separated into two groups based on the IFN-β status of individual cells. **D-F, I-J.** BC3-
1006 IFN-βp-tdTomato reporter cells were treated with 20 ng/ml TPA for 48 hours to induce
1007 the lytic cycle ("lytic (+TPA)"), 10 μM of the pan-caspase inhibitor IDN-6556 ("casp-i"),
1008 and/or a cocktail of antibodies against type I IFNs and their receptor ("anti-IFN Abs") to
1009 block IFN-β paracrine signaling. Protein was isolated from BC3-IFN-βp-tdTomato
1010 reporter cells without sorting ("bulk"), or after sorting the lytic+casp-i+anti-IFN Abs
1011 based on tdTomato expression. Western blots were probed for ATF2 (**D**), c-Jun (**D**), or
1012 total RelA and phosphorylated RelA (Ser536) (**I**) and β-actin as a loading control. Levels
1013 of ATF2 (**E**) and c-Jun (**F**) in sorted samples were quantified from the western blots,
1014 normalized to β-actin, and plotted relative to bulk lytic+casp-i+ anti-IFN Abs samples.
1015 Levels of phosphorylated RelA (Ser536) (**J**) were quantified by normalizing to total RelA
1016 and plotted relative to bulk lytic+casp-i+ anti-IFN Abs samples. **G, H, K.** KSHV-negative
1017 BJAB cells were treated with vehicle, 20 ng/ml TPA and/or 10 μM of the pan-caspase

1018 inhibitor IDN-6556 (“casp-i”) for 48 hrs. Protein was isolated and stained for ATF2 (**G**),
1019 c-Jun (**H**), phosphorylated (Ser536) and total RelA (**K**), and β-actin as a loading control.
1020 Images are representative of 4 replicates (**D**), 3 replicates (**I**), or 2 replicates (**G, H, K**).
1021 ns = $p>0.05$, * = $p<0.05$, ** = $p<0.01$, One-Way ANOVA followed by Tukey’s post hoc
1022 multiple comparisons test.
1023
1024 **Figure 6. Model of regulation of heterogeneous IFN-β expression by components**
1025 **of the IFN-β enhanceosome.** *(Left)* In the rare cells that induce IFN-β during viral
1026 infection as “first responders”, there are high levels of the AP-1 factor ATF2 and both
1027 the NF-κB subunit RelA and IRF3 become phosphorylated in response to infection. This
1028 results in the formation of the IFN-β enhanceosome and IFN-β and IFN-λ1 transcription.
1029 *(Right)* In the majority of virally infected cells, there are lower amounts of ATF2, and
1030 RelA is not phosphorylated during infection. While IRF3 is still activated, the full IFN-β
1031 enhanceosome does not form and IFN-β and IFN-λ1 are not induced.

Figure 1

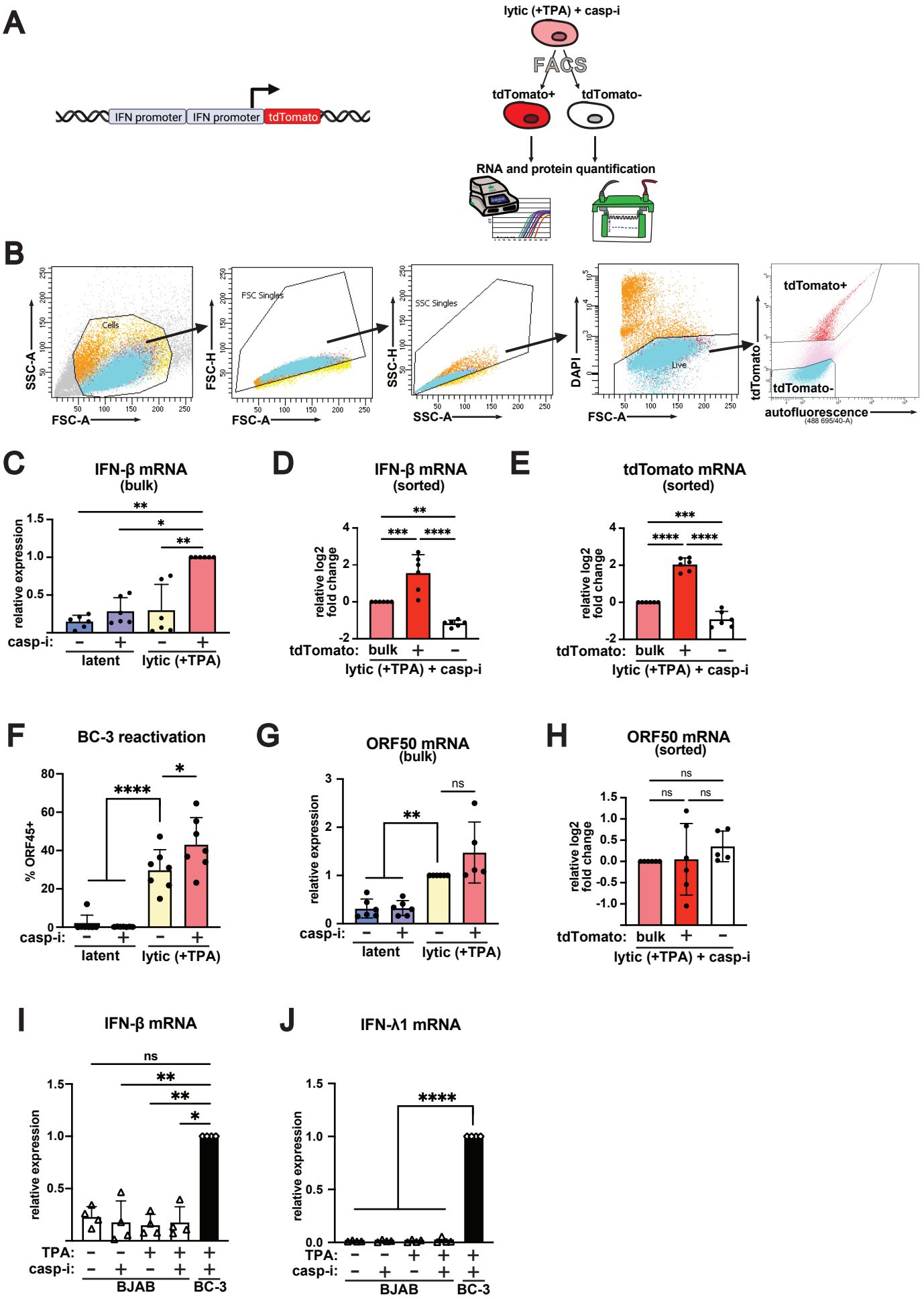
A
IFN promoter
IFN promoter
tdTomato
lytic (+TPA) + casp-i
FACS
tdTomato+
tdTomato-
RNA and protein quantification
B
SSC-A
FSC-A
Cells
FSC-H
FSC Singles
SSC-H
SSC Singles
DAPI
Live
tdTomato
tdTomato+
tdTomato-
autofluorescence
(488 695/40-A)
C
IFN-β mRNA
(bulk)
relative expression
casp-i:
latent
lytic (+TPA)
D
IFN-β mRNA
(sorted)
relative log2 fold change
tdTomato:
bulk
lytic (+TPA) + casp-i
E
tdTomato mRNA
(sorted)
relative log2 fold change
tdTomato:
bulk
lytic (+TPA) + casp-i
F
BC-3 reactivation
% ORF45+
casp-i:
latent
lytic (+TPA)
G
ORF50 mRNA
(bulk)
relative expression
casp-i:
latent
lytic (+TPA)
H
ORF50 mRNA
(sorted)
relative log2 fold change
tdTomato:
bulk
lytic (+TPA) + casp-i
I
IFN-β mRNA
relative expression
TPA:
casp-i:
BJAB
BC-3
J
IFN-λ1 mRNA
relative expression
TPA:
casp-i:
BJAB
BC-3

Figure 1. An IFN-β-promoter driven fluorescent reporter allows isolation of cells expressing high and low levels of IFN-β. A. Diagram of the IFN-βp-tdTomato reporter and sorting strategy. Two copies of the 303 bp minimal promoter sequence for the human IFNB1 gene were cloned in front of the tdTomato fluorophore. This cassette was then introduced in BC-3 cells via lentiviral transduction for stable integration. Cells were sorted based on tdTomato expression and RNA and protein samples were collected from the same experiment. **B-H.** BC3-IFN-βp-tdTomato reporter cells were treated with 20 ng/mL TPA for 48 hours to induce the lytic cycle ("lytic (+TPA)"). Where indicated, the cells were also treated with 10 μM of the pan-caspase inhibitor IDN-6556 ("casp-i"). **B.** Gating strategy for FACS. **C-E**, **G-H**. IFN-β, tdTomato, and ORF50 mRNA levels were measured by RT-qPCR and normalized to 18S rRNA. For **C-E** and **H**, mRNA levels are plotted relative to the lytic+casp-i sample. For **G**, mRNA levels are plotted relative to the lytic sample. **H.** Cells were stained for KSHV ORF45 and analyzed by flow cytometry. **I-J.** KSHV-negative BJAB cells were treated with 20 ng/mL TPA for 48 hours. Where indicated, the cells were also treated with 10 μM of the pan-caspase inhibitor IDN-6556 ("casp-i"). BC-3 cells treated with 20 ng/mL TPA and 10 μM of the pan-caspase inhibitor IDN-6556 ("casp-i") were used as a positive control. IFN-β and IFN- λ1 mRNA levels were measured by RT-qPCR and normalized to 18S rRNA. They are plotted relative to the BC-3 positive control. ns = $p>0.05$, ** = $p<0.01$, *** = $p<0.001$, **** = $p<0.0001$. One-Way ANOVA followed by Dunnett's (C, F, G, I, J) or Tukey's (D, E, H) post hoc multiple comparisons test. $n \geq 4$ for all experiments.

Figure 2

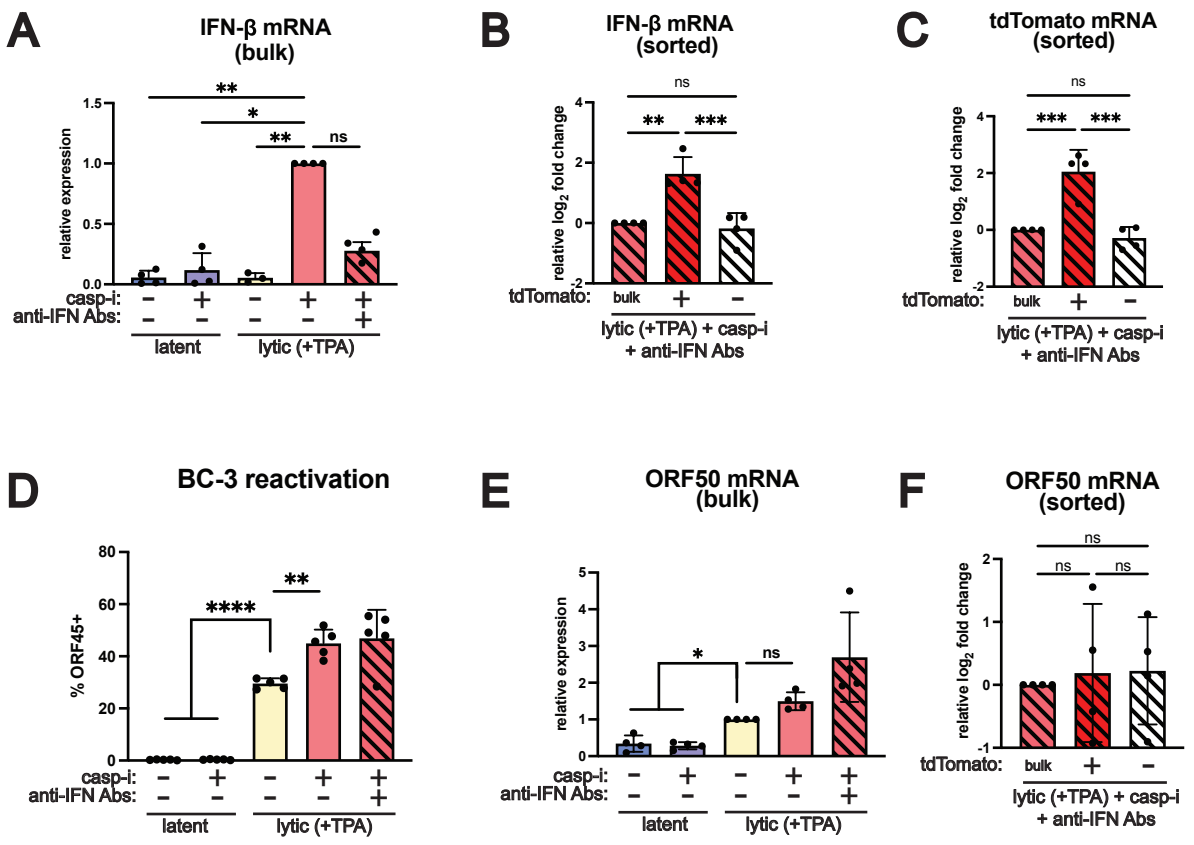

Figure 2. The IFN-β reporter allows isolation of cells expressing high and low levels of IFN-β when paracrine signaling is blocked. BC3-IFN-βp-tdTomato reporter cells were treated with 20 ng/mL TPA for 48 hours to induce the lytic cycle ("lytic (+TPA)"). Where indicated, the cells were also treated with 10 μM of the pan-caspase inhibitor IDN-6556 ("casp-i") and a cocktail of antibodies against type I IFNs and their receptor ("anti-IFN Abs") at 1:2000 dilution. **A-C**, **E-F**. IFN-β, tdTomato, and ORF50 mRNA levels were measured by RT-qPCR and normalized to 18S rRNA. For **A-C** and **F**, mRNA levels are plotted relative to the lytic+casp-i sample. For **E**, mRNA levels are plotted relative to the lytic sample. **D.** Cells were stained for KSHV ORF45 and analyzed by flow cytometry. ns = p>0.05, ** = p<0.01, *** = p<0.001, **** = p<0.0001. One-Way ANOVA followed by Dunnett's (A, D, E) or Tukey's (B, C, F) post hoc multiple comparisons test. n≥ 4 for all experiments.

Figure 3

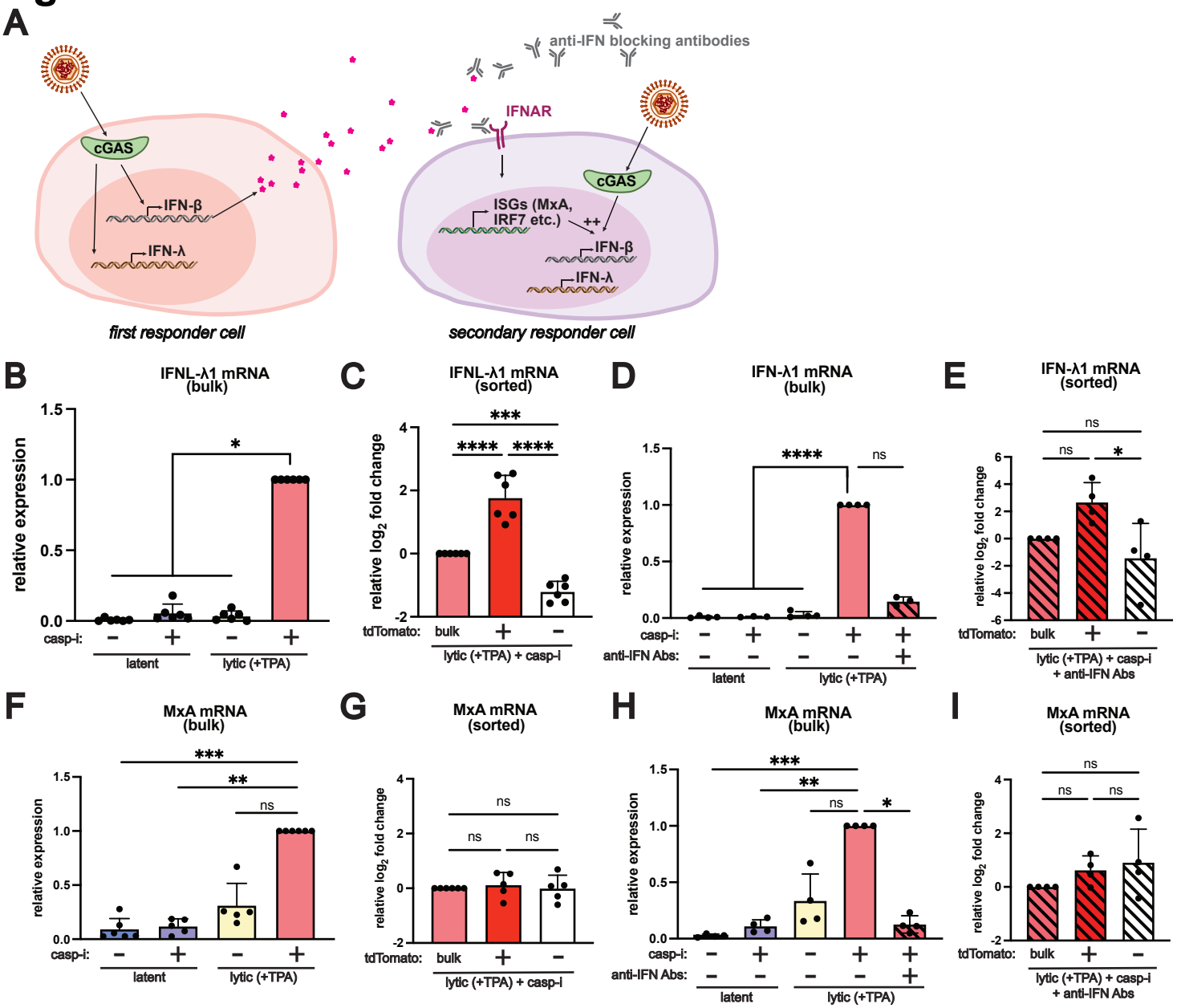

Figure 3. IFN-λ1 and IFN-β are coordinately induced in a subset of cells, pointing to heterogeneity in the induction pathway rather than stochastic noise in expression. A. Diagram of coordinate induction of IFN-β and IFN-λ. In "first responder" cells, IFN-β and IFN-λ are induced in response to infection or lytic reactivation downstream of PRRs. In "secondary responder" cells, ISGs such as MxA and many components of the IFN induction pathway like IRF7 are induced in response to signaling downstream of IFN receptors. Induction of genes like IRF7 potentiates IFN induction in these cells. Anti-IFN antibodies block paracrine signaling from IFN-β to prevent ISG induction and potentiation of IFN induction in secondary responder cells. B-I. BC3-IFN-βp-tdTomato reporter cells were treated with 20 ng/ml TPA for 48 hours to induce the lytic cycle ("lytic (+TPA)"). Where indicated, the cells were also treated with 10 μM of the pan-caspase inhibitor IDN-6556 ("casp-i") and/or a cocktail of antibodies against type I IFNs and their receptor ("anti-IFN Abs") at 1:2000 dilution. IFN-λ1 (B-E) and MxA (F-I) mRNA levels were measured by RT-qPCR and normalized to 18S rRNA. In B-D, and F-H, IFN-λ1 and MxA mRNA levels are plotted relative to the lytic+casp-i sample. In E and I, IFN-λ1 and MxA mRNA levels are plotted relative to the lytic+casp-i+anti-IFN Abs sample. The lytic+casp-i (C, G) or the lytic+casp-i+anti-IFN Abs (E, I) samples were sorted based on tdTomato expression and the fold enrichment in IFN-λ1 (C, E) and MxA (G, I) mRNA levels compared to unsorted ("bulk") samples are plotted in log2 scale. Results in this figure were obtained from the same samples used in Fig. 1 and are thus directly comparable to IFN-β enrichment shown in that Figure. ns = $p>0.05$, * = $p<0.05$, ** = $p<0.01$, **** = $p<0.0001$, One-Way ANOVA followed by Dunnett's (B, D, F, H) or Tukey's (C, E, G, I) post hoc multiple comparisons test. $n \geq 4$ for all experiments.

Figure 4

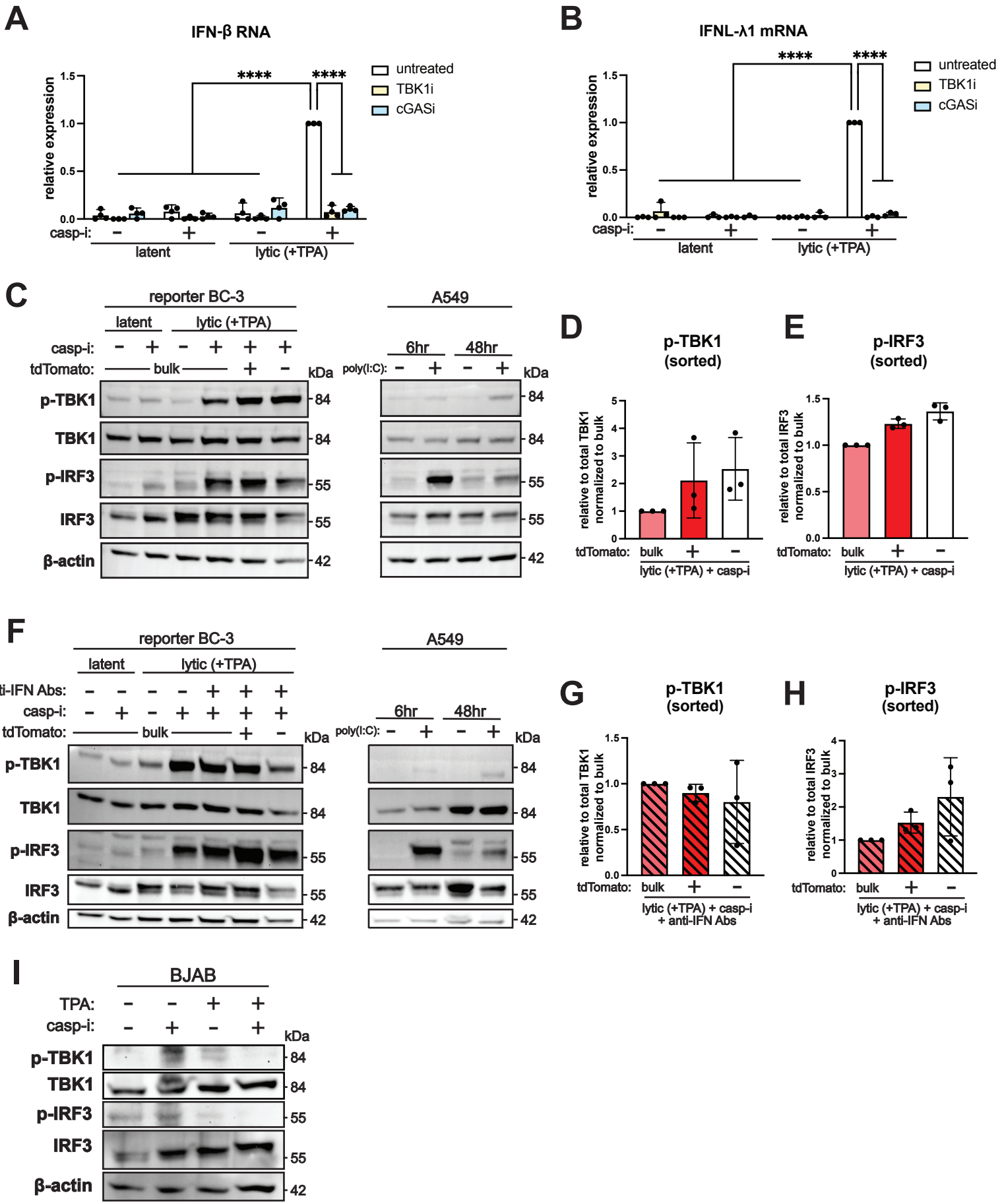
A
IFN-β RNA
relative expression
1.5
1.0
0.5
0.0
****
****
untreated
TBK1i
cGASi
casp-i: − + − +
latent
lytic (+TPA)
B
IFNL-λ1 mRNA
relative expression
****
****
untreated
TBK1i
cGASi
casp-i: − + − +
latent
lytic (+TPA)
C
reporter BC-3
latent
lytic (+TPA)
casp-i: − + − + + +
tdTomato: bulk + −
kDa
p-TBK1 84
TBK1 84
p-IRF3 55
IRF3 55
β-actin 42
A549
6hr
48hr
poly(I:C): − + − +
kDa
84
84
55
55
42
D
p-TBK1
(sorted)
relative to total TBK1
normalized to bulk
5
4
3
2
1
0
tdTomato: bulk + −
lytic (+TPA) + casp-i
E
p-IRF3
(sorted)
relative to total IRF3
normalized to bulk
1.5
1.0
0.5
0.0
tdTomato: bulk + −
lytic (+TPA) + casp-i
F
reporter BC-3
latent
lytic (+TPA)
anti-IFN Abs: − − − − + + +
casp-i: − + − + + + +
tdTomato: bulk + −
kDa
p-TBK1 84
TBK1 84
p-IRF3 55
IRF3 55
β-actin 42
A549
6hr
48hr
poly(I:C): − + − +
kDa
84
84
55
55
42
G
p-TBK1
(sorted)
relative to total TBK1
normalized to bulk
1.5
1.0
0.5
0.0
tdTomato: bulk + −
lytic (+TPA) + casp-i
+ anti-IFN Abs
H
p-IRF3
(sorted)
relative to total IRF3
normalized to bulk
4
3
2
1
0
tdTomato: bulk + −
lytic (+TPA) + casp-i
+ anti-IFN Abs
I
BJAB
TPA: − − + +
casp-i: − + − +
kDa
p-TBK1 84
TBK1 84
p-IRF3 55
IRF3 55
β-actin 42

Figure 4. TBK1 and IRF3 are necessary but not sufficient to direct IFN-β expression, as they are activated even in cells with low IFN-β expression. BC3-IFN-βp-tdTomato reporter cells were treated with 20 ng/ml TPA for 48 hours to induce the lytic cycle ("lytic (+TPA)"). Where indicated, the cells were also treated with 10 μM of the pan-caspase inhibitor IDN-6556 ("casp-i"), 10 μM of the TBK1 inhibitor MRT76307 ("TBK1i"), 10 μM of the cGAS inhibitor G140 ("cGASi"), and/or a cocktail of antibodies against type I IFNs and their receptor ("anti-IFN Abs") at 1:2000 dilution. **A-B.** IFN-β and IFN-λ1 mRNA levels were measured by qRT-PCR and normalized to 18S rRNA. The expression levels are plotted relative to "untreated" lytic+casp-i samples that did not receive TBK1i or cGASi treatment for each experiment. n=3. **** = $p<0.0001$. Two-Way ANOVA followed by Tukey's post hoc multiple comparisons test. **B-H.** Protein lysates were probed for phosphorylated IRF3 (Ser386), total IRF3, phosphorylated TBK1 (Ser172), total TBK1, and β-actin as a loading control. As a positive control for IRF3 and TBK1 activation/phosphorylation, A549 cells were treated with poly(I:C) for 6 and 48 hours before protein lysates were collected. Protein was isolated from treated BC3-IFN-βp-tdTomato reporter cells without sorting ("bulk"), or after sorting the lytic+casp-i (**C-E**) or lytic+casp-i+anti-IFN Abs (**F-H**) sample based on tdTomato expression (**D-E**, **G-H**). Western blot for phosphorylated TBK1 and phosphorylated IRF3 for bulk lytic+casp-i or lytic+casp-i+anti-IFN Abs treated samples and sorted tdTomato+ and tdTomato- samples were quantified by normalizing the density of phosphorylated protein to unphosphorylated protein bands. Phosphorylation levels are plotted relative to the bulk lytic+casp-i or lytic+casp-i+anti-IFN Abs treated samples. **I.** KSHV-negative BJAB cells were treated with vehicle, 20 ng/ml TPA, and/or 10 μM of the pan-caspase inhibitor IDN-6556 ("casp-i") for 48 hours. Protein was isolated and stained for phosphorylated TBK1, total TBK1, phosphorylated IRF3, and total IRF3. Images shown are representative of 3 replicates (**A-H**) or 2 replicates (**I**).

Figure 5

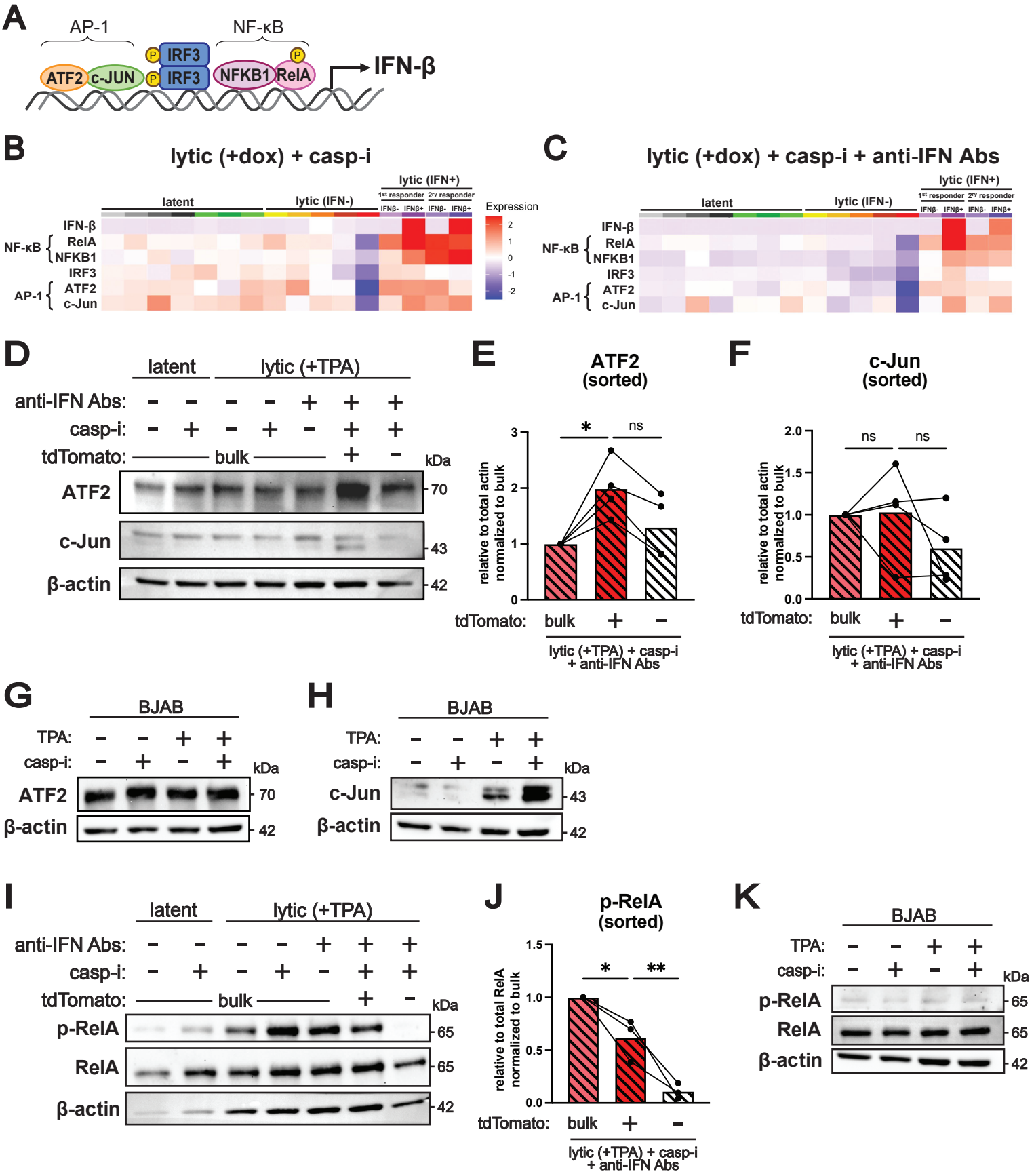
A
AP-1
NF-κB
IRF3
IRF3
ATF2
c-JUN
NFKB1
RelA
IFN-β
B
lytic (+dox) + casp-i
latent
lytic (IFN-)
lytic (IFN+)
1st responder
2ry responder
IFNβ-
IFNβ+
Expression
IFN-β
NF-κB
RelA
NFKB1
IRF3
AP-1
ATF2
c-Jun
C
lytic (+dox) + casp-i + anti-IFN Abs
D
latent
lytic (+TPA)
anti-IFN Abs:
casp-i:
tdTomato:
bulk
kDa
ATF2
c-Jun
β-actin
70
43
42
E
ATF2
(sorted)
relative to total actin normalized to bulk
tdTomato:
bulk
lytic (+TPA) + casp-i + anti-IFN Abs
F
c-Jun
(sorted)
G
BJAB
TPA:
casp-i:
ATF2
β-actin
H
c-Jun
I
p-RelA
RelA
J
p-RelA
(sorted)
relative to total RelA normalized to bulk
K
65

Figure 5. Levels of the AP-1 subunit ATF2 and phosphorylation of the NF-κB subunit RelA are higher in cells with high IFN-β expression. A. Diagram of the IFN-β enhanceosome and its position on the IFN-β promoter. In the IFN-β enhanceosome, NF-κB is composed of subunits NFKB1 (p50) and RelA, and AP-1 is composed of subunits ATF2 and c-Jun. **B-C.** Re-analysis of single-cell RNA sequencing (scRNA-seq) data in Tabtieng, Lent, et al 2022. iSLK.219 cells were treated with 1 μg/mL doxycycline for 4 days to induce the lytic cycle ("lytic"). The cells were also treated with 10 μM of the pan-caspase inhibitor IDN-6556 ("casp-i"), as well as a mixture of antibodies against type I IFNs and its receptor ("anti-IFN Abs") (**C** only) to block IFN-β paracrine signaling. The average mRNA levels of genes in the IFN-β enhanceosome from the scRNA-seq data are shown for each of the 12 clusters of cells identified by the original analysis (indicated by different colors above the heatmap). Clusters were classified as "latent". "lytic", or "lytic IFN-β-positive" based on the pattern of viral genes they expressed and whether they also expressed IFN-β. The "lytic IFN-β-positive" clusters were further separated into two groups based on the IFN-β status of individual cells. **D-F**, **I-J.** BC3-IFN-βp-tdTomato reporter cells were treated with 20 ng/ml TPA for 48 hours to induce the lytic cycle ("lytic (+TPA)"), 10 μM of the pan-caspase inhibitor IDN-6556 ("casp-i"), and/or a cocktail of antibodies against type I IFNs and their receptor ("anti-IFN Abs") to block IFN-β paracrine signaling. Protein was isolated from BC3-IFN-βp-tdTomato reporter cells without sorting ("bulk"), or after sorting the lytic+casp-i+anti-IFN Abs based on tdTomato expression. Western blots were probed for ATF2 (**D**), c-Jun (**D**), or total RelA and phosphorylated RelA (Ser536) (**I**) and β-actin as a loading control. Levels of ATF2 (**E**) and c-Jun (**F**) in sorted samples were quantified from the western blots, normalized to β-actin, and plotted relative to bulk lytic+casp-i+ anti-IFN Abs samples. Levels of phosphorylated RelA (Ser536) (**J**) were quantified by normalizing to total RelA and plotted relative to bulk lytic+casp-i+ anti-IFN Abs samples. **G, H, K.** KSHV-negative BJAB cells were treated with vehicle, 20 ng/ml TPA and/or 10 μM of the pan-caspase inhibitor IDN-6556 ("casp-i") for 48 hrs. Protein was isolated and stained for ATF2 (**G**), c-Jun (**H**), phosphorylated (Ser536) and total RelA (**K**), and β-actin as a loading control. Images are representative of 4 replicates (**D**), 3 replicates (**I**), or 2 replicates (**G, H, K**). ns = $p>0.05$, * = $p<0.05$, ** = $p<0.01$, One-Way ANOVA followed by Tukey's post hoc multiple comparisons test.

Figure 6

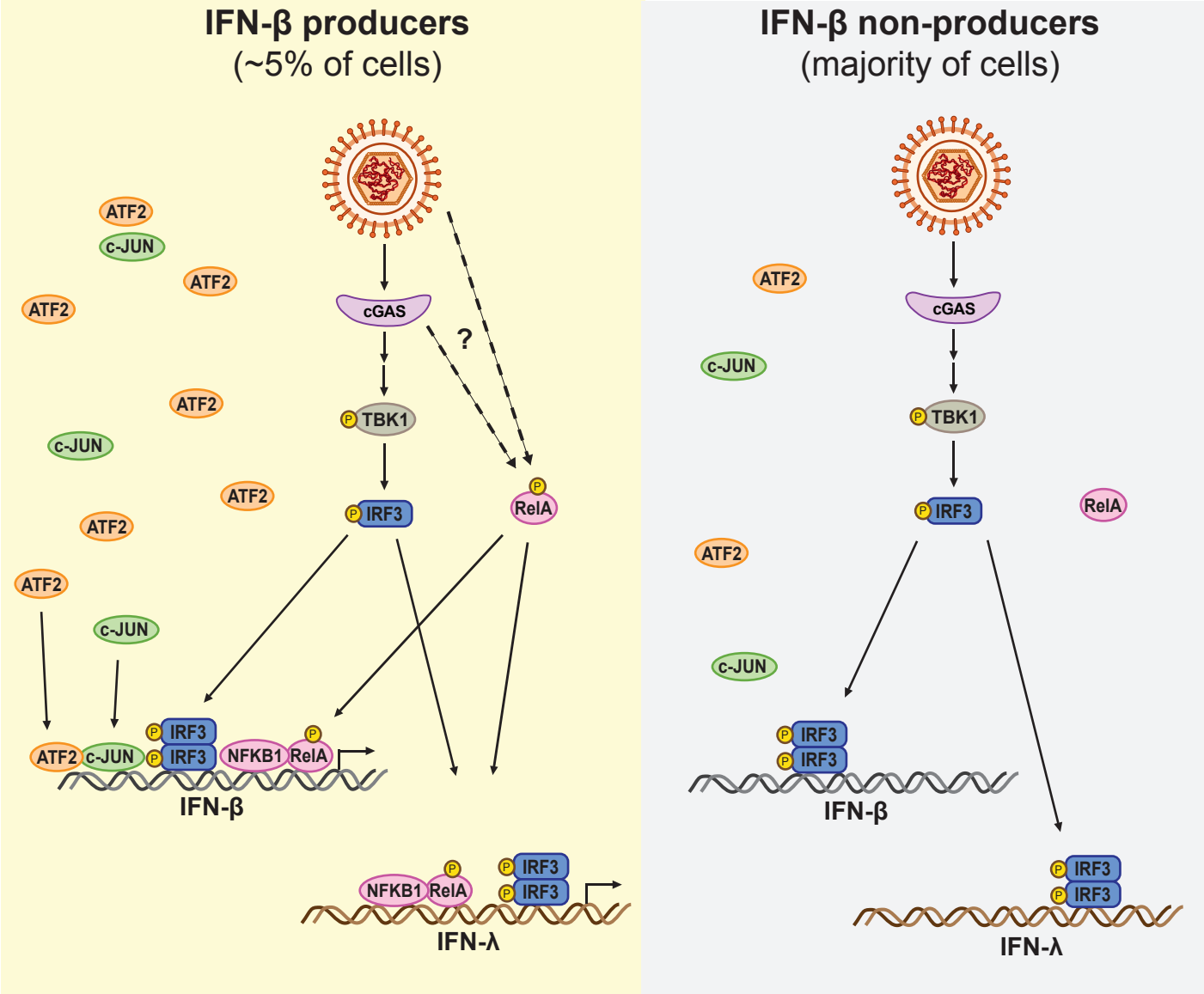

Figure 6. Model of regulation of heterogeneous IFN-β expression by components of the IFN-β enhanceosome. (*Left*) In the rare cells that induce IFN-β during viral infection as "first responders", there are high levels of the AP-1 factor ATF2 and both the NF-κB subunit RelA and IRF3 become phosphorylated in response to infection. This results in the formation of the IFN-β enhanceosome and IFN-β and IFN-λ1 transcription. (*Right*) In the majority of virally infected cells, there are lower amounts of ATF2, and RelA is not phosphorylated during infection. While IRF3 is still activated, the full IFN-β enhanceosome does not form and IFN-β and IFN-λ1 are not induced.